Addis Ababa University
አዲስ፡አበባ፡ዩኒቨርሲቲ
SEEK WISDOM, ELEVATE YOUR INTELLECT AND SERVE HUMANITY !

ADDIS ABABA UNIVERSITY

INSTITUTE OF TECHNOLOGY

SCHOOL OF MECHANICAL AND INDUSTRIAL ENGINEERING

Investigating an Interaction between Rail Vehicle Dynamics and Track Alignment of Addis Ababa Light Rail Train

A Thesis Submitted to the School of Graduate Studies of Addis Ababa institute of Technology in Partial Fulfillment of the Requirement for the Degree of Masters of Science in Mechanical Engineering (Rolling stock Engineering)

By

Melkamu Ashenafi

Advisor

Ato. Habtamu Tekubet (M.SC.)

July 2017

Addis Ababa, Ethiopia

Addis Ababa University
አዲስ፡አበባ፡ዩኒቨርሲቲ
SEEK WISDOM, ELEVATE YOUR INTELLECT AND SERVE HUMANITY !

Declaration

This is to certify that the thesis prepared by Melkamu Ashenafi entitled: Investigating an Interaction between Rail Vehicle Dynamics and Track Alignment of Addis Ababa Light Rail Train submitted in the fulfillment of the requirements for the degree of masters of Science in mechanical engineering (Rolling stock Engineering) compiles with the regulations of the university and meets the accepted standards with respect to original qualification.

Done by Melkamu Ashenafi
Julay 2017

Melkamu Ashenafi	______________________	_______________
Student	Signature	Date

Approved by Board of Examiners:

HabtamuTekubet (MSc)	______________________	_______________
Advisor	Signature	Date
Hairedin Ismael (MSc)	______________________	_______________
Internal Examiner	Signature	Date
Araya Abera (MSc)	______________________	_______________
External Examiner	Signature	Date
Daniel Tilahun (Dr)	______________________	_______________
Railway center head	Signature	Date

Acknowledgement

At first I would like to thank God strengthening me to do with great moral and accomplish within the limited time of the paper.

Conducting this paper research from thesis proposal preparation, data collection, and to the final write up of the thesis could have not been met if it were not included the assistance of my advisor Ato Habtamu Tikubet for his endogenous support, timely guidance, Critical comments, patience, and encouragement throughout the any activities of my thesis.

I would also like to thank some staffs of Ethiopia Railways Corporation particularly Ato Dawit (AALRT infrastructure maintenance director), Ato Nahom (AALRT infrastructure maintenance expert), Ato Muluken (AALRT rolling stock maintenance director), my classmates, for providing me the necessary data and sharing basic ideas which are used in the development of my paper and I would also like to thank Ethiopian Railways Corporation (ERC) for financial support of my education.

Finally i would like to express a sincerely gratitude to my family for their understanding, support and encouragement in my life.

Abstract

This thesis examines the effect of vehicle dynamics on both vertical and lateral deterioration of the track alignment. The track system, the measurements of the track geometry and the definition of the track quality are explained in detail. The background study forms fundamental knowledge for the vehicle-track lateral dynamic interaction study. A review of current researches in the field of vertical and lateral railway track deterioration is presented in order to establish a better understanding of track deterioration mechanisms, highlighting the weakness and limitations of these studies.

Based on the background and the reviews done in the field, the statistical analysis is done and provides a better understanding of three aspects of track lateral irregularities: the relationship between vertical and lateral irregularities, the relationship between track curvature and track lateral irregularity and the change in track lateral deterioration over time.

The paper describes statistical studies of track deterioration, as well as the development and validation of a vehicle-track dynamic interaction model so that making the effective control and reduction of the lateral deterioration achievable and the vertical and lateral track irregularity magnitudes are clearly correlated. The model indicates the mechanisms influencing track deterioration both vertically and laterally which provides effective solutions in consideration of vehicles, wheel-rail contact and the track system.

Key words: -Rail Vehicle, Dynamics, Lateral Misalignment, Interaction, Irregularity, power spectral density and vehicle loading.

Table of contents

List of Tables

List of Figures

List of symbols used

Symbols	Definitions
L	Lateral loading
V	Vertical loading
TQI	Track Quality Index
ABA	Axle Box Acceleration
SD	Standard Deviation
PSD	Power Spectral Density
RMS	Root Mean Square
CWR	Continuously Welded Rail
TRC	Track recorded coach
$\mathbf{S_v(\omega)}$	Vertical track irregularity
$\mathbf{S_S(\omega)}$	Lateral track irregularity
A	Roughness constant ($m^2.rad.m^{-1}$)
$\boldsymbol{\omega}$	Irregularity frequencies ($rad.m^{-1}$)
V	Speed of the model vehicle
$\mathbf{t_1}$	Starting time of the test
$\mathbf{t_2}$	Ending time of the test
a(t)	Time series of acceleration
$\boldsymbol{\gamma_a}$	RMS value
AALRT	Addis Ababa light rail train

MBS	Multi body system
ERC	Ethiopian Railway Corporation
DOF	Degree of freedom
ORE	Office Research Experiments
BRR	British Rail Research
TLV	Track loading vehicle
N_y	Bearing capacity factor
S_y	Shape factor
B	Foundation width
L	Foundation length
Γ	Bulk unit weight of ballast
u	pore water pressure
FEA	Finite Element Analysis
r	Correlation coefficient
S	Average irregularity growth rate
T	Traffic tonnage
V	Average running speed
M	Structure factor
L	Joint influence factor
NWHPY	Number of working hours per year
Y_r	Right rail deviation

Y_l	Left rail deviation
M	Mass matrix
K	Stiffness matrix
C	Damping matrix
L	Track length
E	Young's modulus
I	Moment of inertia
m_r	Mass of rail
Mc	Motored coach
T	Trailer

Chapter one

1.1. Introduction

Track condition has a big influence on the behavior of the train-track system in terms of ride safety, maintenance and passenger comfort. However, it is physically impossible to eliminate track irregularities. It is therefore important to understand the mechanism of track deterioration and predict the development of track irregularities to reduce the life-cycle cost of the railway system. The track system supports the loads due to the passage of vehicles, spreads the load into the ground, provides guidance to the traffic and resists traction and braking forces. It generally consists of the subgrade, ballast, sleepers, rail fastenings and the rail, as shown in Figure 1-1 below (1).

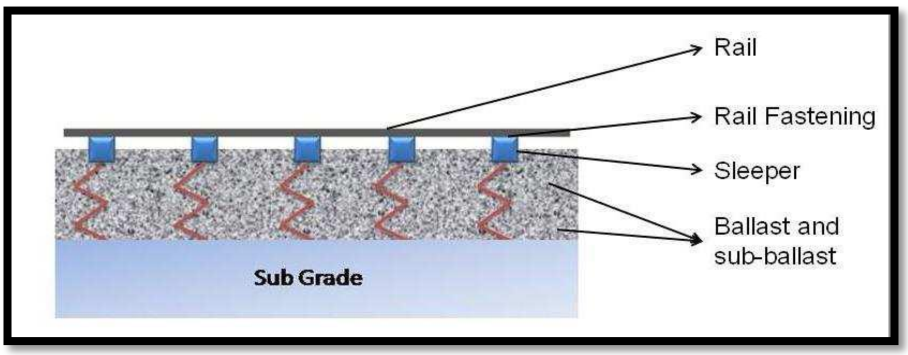

Figure 1.1.1 track system components

Track lateral irregularity: Track lateral irregularities are usually corrected before they have a big influence on ride comfort or safety mainly because the vertical irregularities are much bigger and grow much faster, and hence need maintenance operations more frequently. The growth of lateral misalignments may be caused by a high L/V loading ratio, an increase in longitudinal forces, track dynamic uplift due to high vertical loads, etc. The growth may become stable after many loading cycles or keep increasing until there is a risk of buckling, which can cause derailment. The initial lateral misalignment tolerance for high speed newly installed track is between 1 and 4 mm, and the maximum allowable before maintenance required is 4 mm for high speed lines (2). The recorded track lateral irregularities are low pass filtered either at 35 m or 70 m wavelength, and any longer wavelength irregularity may be obtained from the curvature measurement.

Track geometry and measurement: Good track condition is important in ensuring more efficient train-track system in terms of the safe running, low maintenance and good passenger comfort. However, it is physically impossible to completely eliminate all track irregularities in practice. Track irregularities are characterized in different ways and described by their different wavelengths. To achieve a quantitative assessment of the condition of the track system, it is necessary to be able to describe the track by measureable parameters. The fundamental track geometry parameters are the track alignment in vertical, horizontal and twist directions, track gauge, cant, curvature, gradient, and rail profile but in this paper track vertical and lateral or gauge and curvature parameters are going to be studied. The track geometry plays an essential role in the ride quality and safety of operations, and it degrades under repeated dynamic loading from the passing traffic (3).

Different countries have their own standards when it comes to describing track geometry. The track quality in China is described using a Track Quality Index (TQI), which is the sum of standard deviations of seven track irregularity parameters. These seven parameters are left rail vertical profile, right rail vertical profile, left rail alignment, right rail alignment, gauge, cross level and track twist (4).

In this thesis left rail vertical profile, left rail alignment, gauge or lateral rail parameters are going to be studied.

Portable, manually driven devices give information on a relatively short length of track (5). Axle Box Acceleration (ABA) measurement uses the accelerations due to the wheel-rail interaction, as shown in Figure 1-2, and converts the accelerations to displacements by double integration. The mid-chord offset method is currently the mainstream method to measure vertical and horizontal track displacements, which uses three measuring axes arranged inline (6).

The track is dynamically excited through two oscillating masses above an ordinary wheel axle of a freight wagon. The latter two measurement methods are able to highlight defects like ballast fouling, ballast settlement, subgrade failure and problems related to embankments (7).

Description of track quality based on measured irregularities: Measuring the size of track irregularities can be used to characterize the quality of the track with respect to different requirements such as the speed category or engineering maintenance activities. This section describes the various mathematical tools used to characterize track quality such as Standard

Deviation (SD) which is the most common way to describe the smoothness of the track that shows the amount of track variation from its mean value. This form of analysis provides track quality indices (8).

Power Spectral Density (PSD) plot: shows the distribution of the power over different frequencies. Track vertical irregularities are defined by using a PSD function in the track irregularity model which predicts the value of peak amplitudes for a given track length. The PSD method is widely used in different countries to analyze track irregularities (9).

Root Mean Square (RMS) value has been used to describe track irregularities in a rail surface corrugation study. RMS value of the unsprung mass acceleration describes the track irregularity indirectly (10).

Track vertical irregularity: Track measurement contains irregularities of varying wavelengths, typically ranging from approximately 30 mm to over 70 m (or 150 m in case of high speed measurement). The distribution of track irregularities can be periodic, random or discrete. Railhead corrugations or cross-beam and sleeper effects are considered as periodic irregularities, which can cause significant vehicle vibrations (11).

1.2. Railway track system

The track system supports the loads due to the passage of vehicles, spreads the load into the ground, provides guidance to the traffic and resists traction and braking forces. It generally consists of the subgrade, ballast, sleepers, rail fastenings and the rail. The function of the rail is to guide and support the vehicle. The rail fastenings secure the rail to the sleepers to maintain the gauge, transfer the dynamic load from the wheel-rail interface to the sleeper and provide electrical isolation between the rail and the sleeper. The ballast layer holds the sleepers in position, distributes the forces from sleepers to subgrade, provides some resilience to the system and aids drainage. The subgrade, which is the original ground that the track system is constructed on, absorbs all the forces from the ballast. There may also be a geotextile layer and or a capping layer between the ballast and the subgrade depending on the properties of the subgrade.

1.2.1. Rails

The rail has the function of supporting and guiding the vehicles running on it. Originally, the rails were short in length, 18 m were common, and were joined using bolts and fishplates at the ends. Over a large number of loading cycles, it was found that the joints developed dips due to the inherent weakness of the joint. As the joint dip increases, so-called P2 forces, which are a relatively low frequency dynamic forces, occur when the wheel and rail vibrate on the ballast (3). P2 forces cause rapid deterioration of the track quality. Continuously Welded Rail (CWR) eliminates the joints by welding the rail ends together into much longer lengths. CWR substantially reduces rail maintenance, in that the damage occurring to the rail ends and misalignment of the rails are minimized (4).Thus, an improved ride quality is provided and the life of all track components is extended.

There are many different rail cross-section profiles and different wheel and rail profiles generate different conicity that in turn influences the vehicle hunting stability (5), and wheel and rail wear (6), It is generally considered essential to achieve an optimal combination of wheel and rail profiles (7). The dynamic performance of the vehicles is largely determined by the interaction between the wheel and rail, which has been extensively studied, e.g. (8, 9). Grinding is a typical maintenance method used to control surface fatigue (10) and keeps the rail surface in good condition. The interface between rail and wheel connects the railway vehicles with the track system, thus the understanding of it is important in the study of vehicle dynamics and track lateral alignment.

1.2.2. Rail fastenings

Rail fastening systems fix the rail to the sleeper, restraining the rail against longitudinal movement and preventing it from overturning (11). The rail fastening systems also transfer the vertical, horizontal and longitudinal forces from the rail to the sleeper. Different types of rail fastenings may be selected based on a number of aspects such as: cost, installation requirements and behavior. Although there are numerous types of modern rail fastening systems, they have similar fundamental functions which are:

- To secure the rails to the sleepers and maintain the gauge
- To maintain the lateral, vertical and longitudinal position of the rail, thereby
- preventing it from overturning and creeping longitudinally
- To transfer the wheel load from the rail to the sleeper
- To provide electrical isolation between rail and the sleeper
- To provide vibration isolation

With the development of the railways, the fastening system has been through significant changes. In the early years, fastenings were mainly non-resilient, known as direct fastenings. Rail spikes and rail chairs are widely used where the rails are rigidly fixed to the sleeper. Non-resilient rail fastenings have the advantages of low cost and easy replacement in case of failure. However, the fastening, sleeper and ballast are all subject to vibration forces which may give rise to fatigue problems. The operating speed of trains on track laid with non-resilient fastenings tends to be relatively slow, and maintenance is more expensive due to the increased forces transmitted to the track system (12). Direct contact between the rail foot and sleeper can also cause severe damage to timber sleepers (13). An increasing requirement for higher operating speeds and lower maintenance costs means that these systems are no longer installed in modern track.

1.2.3. Sleepers

Originally, timber sleepers were used as this was the only viable material available at the time. Pre-stressed concrete sleepers were developed and introduced during the Second World War due to a shortage of timber. Since that time, concrete sleepers have become the standard sleeper used today. Timber sleepers are still used in certain applications due to their greater flexibility, which provides superior load spreading over concrete. Steel sleepers have also been developed as an alternative to concrete, as they are lighter in weight, easy to transport due to their stack ability and the fact that they allow a lower track form height, which makes them suitable for use in loading gauge enhancement projects. Both sleepers and rail fastenings hold the rail at an angle to match the wheel and rail contact angle, such as 1:20 and 1:40 (14).

Two types of typical concrete sleepers are twin block sleeper and mono-block sleeper (15).

Sleepers support the rails vertically, laterally and longitudinally by sitting inside the ballast layer. There are three contact surfaces between the sleeper and ballast: the sleeper base, the sides of the sleepers and the sleeper ends. It is understandable that the more friction force is provided by the ballast, the more stable the track system will be. Therefore, the shape and mass of the sleeper are significant contributors to the stability of the track system.

1.2.4. Ballast

Ballast is a permeable, granular and angular shaped material, and the selection of ballast type usually depends on the material that can be found locally. However the material must be robust enough to withstand the loads from passing traffic without disintegrating, hence granite is the most popular ballast material used in the UK on mainline railways. The ballast material, to some extent, determines the drainage capability, stability and maintenance requirement of the track. Most railway authorities allow 400 to 500kPa pressure on the ballast Ballast is classified into four types by function and location (16).

- Crib ballast is located between sleepers, providing mainly longitudinal resistance and some lateral resistance.
- Shoulder ballast is positioned at the end of the sleepers, giving sufficient lateral resistance to the sleepers.
- Top and sub ballast, also known as load bearing ballast, mainly support the sleepers vertically. The sub-ballast has a smaller size than the top ballast, and lies between the top ballast layer and the subgrade. It can provide a more stable and drained support to the top ballast. The thickness of top and sub ballast is an important factor in the ballast design.

The important functions of ballast are:

- The ballast distributes the load from the sleepers to the subgrade at an acceptable level.
- Ballast provides sufficient drainage.
- The ballast holds the sleepers in place by resisting the vertical, lateral and longitudinal forces caused by the wheel loads.
- The ballast also provides some resilience to the track system.

1.2.5. Description of track quality based on measured irregularities

Measuring the size of track irregularities can be used to characterize the quality of the track with respect to different requirements such as the speed category or engineering maintenance activities. This section describes the various mathematical tools used to characterize track quality.

1.2.6. Standard Deviation (SD)

SD is the most common way to describe the smoothness of the track, which shows an amount of track variation from its mean value.

"Standard deviation is a universally used scientific measure of the variation of a random process. Track profiles have been found to be sufficiently similar statistical properties to random processes to enable a measure of the magnitude of track irregularities to be obtained from the standard deviation of the vertical and horizontal profile data. This form of analysis provides track quality indices (21).

SD can be calculated using the equation shown below:

$$\sigma = \sqrt{\frac{1}{m}\sum(a_1 - a)^2} \qquad \text{Equation 1.2-1}$$

Where, a…mean value, a_1...sample value and m…total number of values.

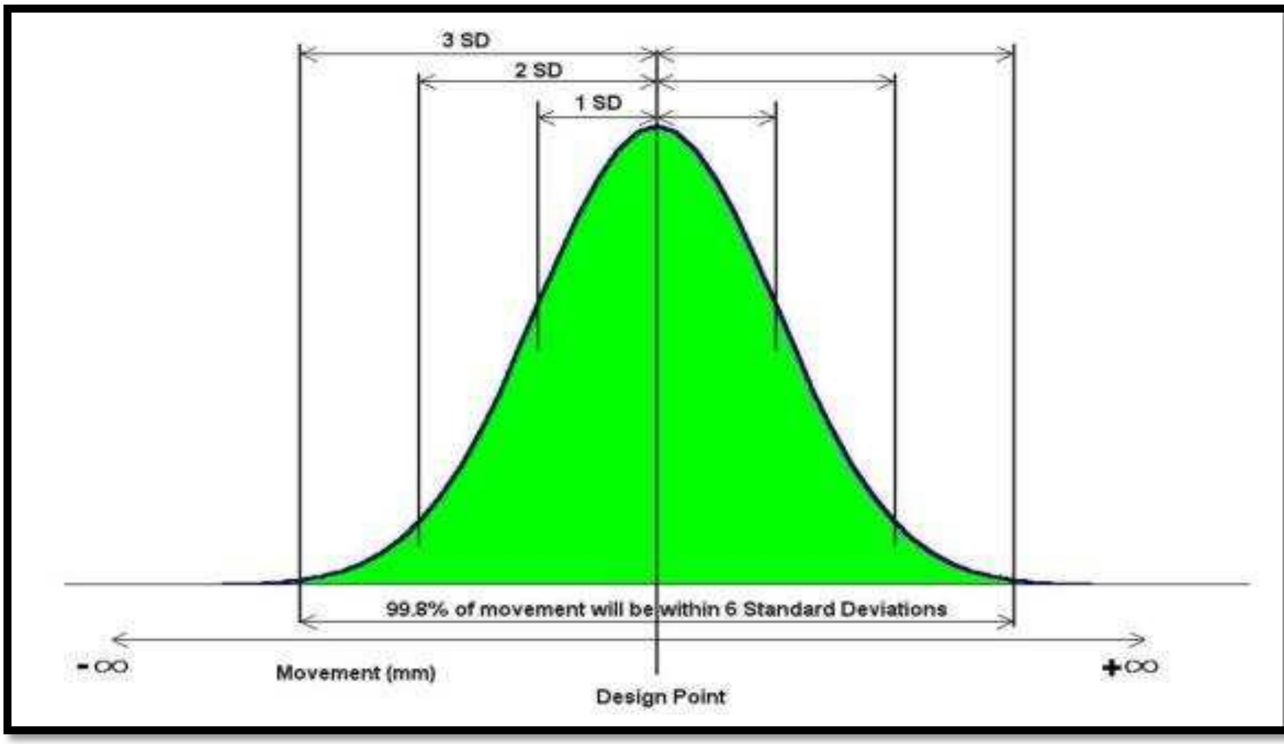

Figure 1.2.1 standard deviation plot

There are two drawbacks in using the SD to describe track irregularities. Firstly, there will be a difference between the ideal SD curve and reality. Also, although a single large discrete defect can lead to derailment, it will not significantly affect the SD of the total track profile. This is why the current UK and EN standard also specify limits on maximum values.

1.2.7. Power Spectral Density (PSD) plot

The distribution of track irregularities can be shown in the form of PSD plot, which shows the distribution of the power over different frequencies. The vertical axis represents the power in each frequency band, while the horizontal axis represents a spatial frequency which is always described by cycle/m. The ideal power spectrum of the track is shown below.

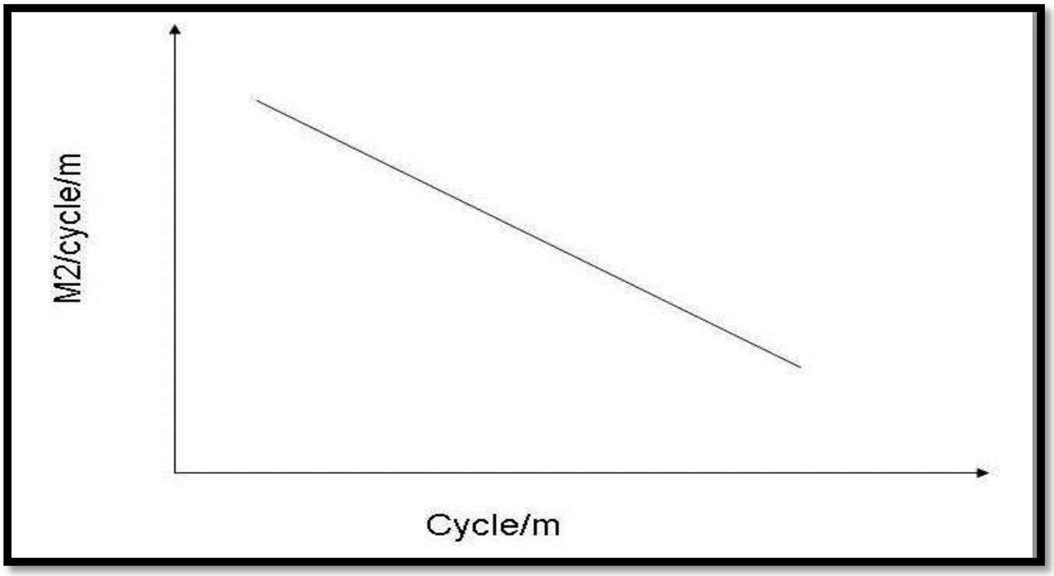

Figure 1.2.2 power spectral density plot

Track vertical irregularities are defined by using a PSD function in the track irregularity model which predicts the value of peak amplitudes for a given track length (22). The PSD method is widely used in different countries to analyze track irregularities. The American Federal Railroad Administration (FRA) collected a large amount of data in order summarize the track irregularities PSD, the equations for which are below (23).

Track vertical irregularity PSD:

$$S_v(\omega) = \frac{kA_v\omega_c{}^2V}{\omega^2(\omega^2-\omega_c{}^2)} \quad \text{Equation 1.2-2}$$

Track lateral irregularity PSD:

$$S_S(\omega) = \frac{kA_S\omega_c{}^2V}{\omega^2(\omega^2-\omega_c{}^2)} \quad \text{Equation 1.2-3}$$

Where, S(ω)… track irregularity PSD (mm^2.m.cycle); A…….. Roughness constant (m^2.rad.m^{-1}); ω…….. Irregularity frequencies (rad.m^{-1}), V …..Speed of the model vehicle and k…constant parameter, usually is 0.25.

1.2.8. Versine

A versine is the distance of the mid-chord offset from a curvature [34. It is easy to measure and calculate, and is sometimes used to describe track irregularities.

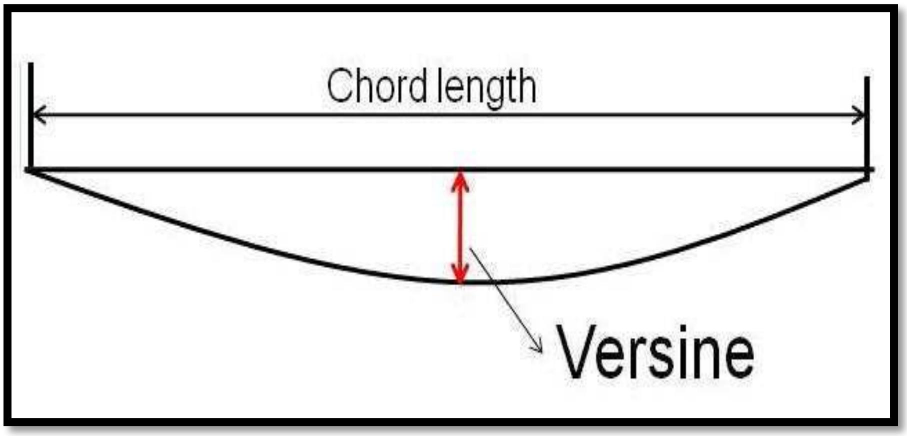

Figure 1.2.3 versine diagram

1.2.9. Root Mean Square (RMS) value

The RMS value has been used to describe track irregularities in a rail surface corrugation study (24). The vertical unsprung-mass acceleration of an axle box induced by the track irregularities is measured. It is a good way of measuring quantities varying both positively and negatively from the mean value, such as track irregularities. RMS value of the unsprung mass acceleration describes the track irregularity indirectly.

$$\gamma_a = \sqrt{\frac{1}{t_2 - t_1}\int_{t_1}^{t_2} a^2\,(t)dt} \qquad \text{Equation 1.2-4}$$

Where, t_1… starting time of the test; t_2…ending time of the test and a(t)…time series of acceleration.

1.3. Track vertical irregularity

Track measurement contains irregularities of varying wavelengths, typically ranging from approximately 30 mm to over 70 m (or 150 m in case of high speed measurement) (25).

TRC vehicles measure a point every 0.2 to 0.3m, therefore the TRC data measurement and derived quality assessment are not valid for the wavelength ranges mentioned above.

Therefore, corrugations and short wavelength irregularities cannot be measured by a TRC and are not typically modeled using vehicle dynamics.The first study of rail corrugations took place in the late 19th Century (26).

Rail corrugations can lead to a number of serious issues under many load cycles, such as the track settlement resulting in a loss of vertical track profile, ballast degradation and fastening deterioration. According to Lichberger (27), Grassie and Kalousek (28), and Sato, Matsumoto et al. (29), there are six types of corrugations: Heavy haul corrugation (200-300mm), Light rail corrugation (500-1500mm), Rolling contact fatigue corrugation (150-450mm), Booted sleeper corrugation (45-60mm), Rutting corrugation (50mm for trams), Roaring rail corrugation on high speed lines (25-80mm).

A detailed study of corrugations using numerical methods was undertaken by Jin, Wen et al (30), which illustrates three factors: the periodically varying of rail profile, the stochastic varying of rail profile and the sleeper pitch, have a strong impact on the formation of rail corrugations.

A series of measurements and tests were undertaken in Britain (31), showing that grinding new rail can delay the formation of rail corrugations by 2.5 years, and grinding corrugated rail can significantly reduce the railhead roughness. With increasing train speed, long wave length track irregularities in the range from 20 m to 120 m have a large effect on comfort.

Long wavelength track irregularities can be caused by various factors. The manufacturing process of the rail explains some long wave irregularities. Meanwhile, the variation of the stiffness and geometry of the track support system leads to long wavelength track irregularities.

1.4. Statement of the problem

Rail vehicle - track alignment is one of the basic issues in railway transportation to be studied for the sake of passenger and commodities safety also vehicle goodness. Due to rail vehicle dynamics, loading and unloading variations, curvatures and track slopes, ups and downs developed on top of the rail causes rail irregularities or rail deterioration which leads track misalignments with the rail vehicle (17).

AALRT track lateral and vertical deterioration due to rail vehicle dynamics is not assessed analyzed and predicted in accordance to actual operating data. Therefore this research tries to investigate the practical interaction between rail vehicle dynamics and track alignment specifically for Addis Ababa light rail train (AALRT) North to South line between Stadium and Meshualekiya stations, in which more problems are being observed since the service is started than other parts of the line due to more curves, switches and turnouts.

1.5. Major Objective and scope of the research

The aim of the research is to assess, analyze and predict railway track lateral and vertical deterioration due to rail vehicle dynamics, effects of track curvature on alignments and validate the investigated value with the actual limiting values of deterioration in terms of track loading and running condition for AALRT North to South line in between Stadium and Meshualekiya substations.

1.5.1. Specific objectives

- Analyzing and predicting railway track lateral and vertical deterioration due to rail vehicle motion and analyzing the key factors in the development of vehicle track misalignment.
- Measuring the deterioration of vertical and lateral track geometry, analyzing the effect of curvature on the deterioration of track geometry.
- To establish track deterioration model over time and determining their relationship with track deterioration.
- Comparing the real measured data with SIMPACK model simulations.

1.6. Methodology

The methodologies followed by this study are reviewing different literatures, collecting data and making analysis on the collected data, modeling and model analysis followed by comparisons the analysis on the collected data with the model analysis.

A dynamics of the rail vehicle and track lateral alignment interaction is to be discussed. The data related to track deterioration is be captured by site measurement using gauge and elevation measuring devices. And then the track data is to be analyzed statistically at the first stage in order to establish an empirical curve that describes the track lateral deterioration. The output of the track lateral deterioration, which is the predicted track lateral irregularity growth, can be used as an input as the irregularity data into the vehicle-track model. Therefore, the interaction between the track and the vehicle can be comprehensively modeled. The dynamics of the complete system will be analyzed including lateral and vertical loadings to increase knowledge of the limiting values. Finally conclusions and recommendations will be drawn from the analyzed data and developed track vehicle dynamics model.

1.7. Expected results and limitations of the research

1.7.1. Expected results

At the end of this paper, rail vehicle dynamic interaction and major factors on the development of track misalignment is going to be identified and discussed in detail. Sleeper-ballast interaction analysis followed by track lateral deterioration model will be developed and identification of influential factors is followed by determining their relationship with track vertical and lateral deterioration.

1.7.2. Limitations of the paper

To complete the paper there were many limitations such as lack of money to buy high tech instruments for measuring both vertical and lateral track irregularities, licensed SIMPACK MBS applications and there was not a difficulty in having full rail track and vehicle related parameters due to lack of giving attentions of some staffs in ERC. Shortage of time was also another problem since the paper needs to be given more attention and follow-up continuously to meet the real objective. Even lack of precisely documented data regarding to AALRT was one of the negative impacts for this thesis being completed on time and being done curiously.

Chapter Two

2.1. Literature review

A large part of a railway infrastructure owner's budget is devoted to maintenance. Nowadays, there is a clear trend towards increasing speeds and capacity, meaning that possession time is reduced and the window for maintenance activities becomes highly constrained. More efforts therefore required to understand the mechanisms of track deterioration and to design suitable maintenance strategies. It is important to understand the mechanism of the track deterioration and be able to predict the growth of track irregularities in order to reduce the life-cycle cost of the railway system and help designing new track structures (1).

This paper presents the responses of the railway vehicle and track components in terms of contact forces and displacements. The considered vehicle model is a five-DOF pitch-plane lumped parameter quarter car model supported on two-dimensional track systems comprising three layers. The car body is linked with the vehicle bogie through secondary suspension springs and damper elements, which is further linked to the wheels through primary suspension springs and damper elements. In modeling of the track, the rail is considered as an infinitely long beam discretely supported by a series of springs, dampers and masses representing the elasticity and damping effects of the rail pads, ballasts, and subgrades respectively. The non-linear Hertzian contact theory is employed to accomplish the dynamic interactions between the lumped mass vehicle and the continuous rail. The drastic effect of one wheel flat to the other perfect wheel-rail contact point is also taken into account (12).

2.1.1. Track settlement models

It is recognized that track irregularities are largely caused by uneven track settlement, and uneven track settlement is largely influenced by the bending stiffness of the rail, ballast layer and subgrade deformation and initial track misalignment (13).

Shenton's Track Settlement Model: Shenton investigated several major factors related to track degradation, the dynamic forces, rail irregularities, sleeper spacing, sleeper support, ballast settlement and substructure. A numerical settlement model was developed to forecast the settlements after each loading cycles (14).

Sato's Track settlement model: Sato claims that the settlement of tamped track under many loading cycles can be expressed as $y = \tau(1 - e^{-\alpha x}) + \beta x$ where, y…settlement [mm], x…repeated number of loading or tonnage carried by track, $\tau.\alpha$ and β are coefficients. The first part of the equation: represents the initial settlement of the track directly after tamping, while second part describes the long term settlement (15).

Frohling's track settlement model: Frohling analyzed the differential track settlement in relation to dynamic wheel loading and track support condition. The methodology of the dynamic settlement model is described in detail in Figure 1-3 below. The process of the accumulated ballast deterioration can be used to account for a mix of cyclic loadings at a particular sleeper. However, only ballast settlement is considered, and no ballast degradation is taken into consideration in this model (16).

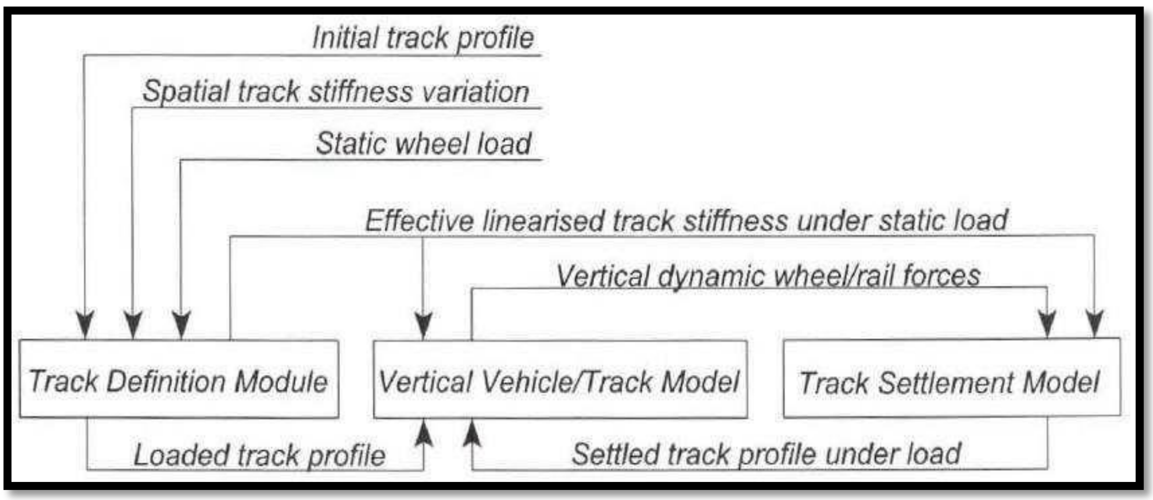

Figure 2.1.1 Interactive dynamic settlement methodology (16)

Track settlement study from ORE: According to ORE (Office for Research and Experiments of the International Union of Railways, UIC) studies by Alva-Hurtado and Selig, the ballast strain after N identical load cycles [mm] can be calculated by:

$e_N = e_1(1 + blogN)$Where, N…number of load cycles b…constant, approximately 0.2 for an individual sleeper, and around 0.43 for the track gride_1…settlement after the first load cycle [mm]. Like Sato's model, this model also consists of those two parts (17).

However, an Australian study by Lonescu et al. has shown that the ORE settlement model is inaccurate under a large number of loading cycles. The track settlement under a large number of loading cycles is stated as:$e_N = e_1N^b$ Where,b…an empirical coefficient. The conclusion of the study is that the trains with high axle loads or high wheel dynamic forces increase track settlement (18).

Ford's track settlement model: One limitation of the ORE model is that there is a precondition of identical loading. Ford has modified this to investigate the varying loading cycles.$e_1$is redefined as which is a curve against the applied stress Δq and failure stress q_f. A new value for N, which is N_e, is determined by:

$N_e = 10^{\frac{\left(\frac{e_N}{e_1'}-1\right)}{b}}$ Where, e_1'…initial permanent strain corresponding to the new load and e…the current value of permanent strain. Unlike Sato's model, the long-term settlement grows logarithmically. The confining stress of the ballast and the ballast failure stress are assumed to be constant, therefore the ballast strain is assumed constant throughout the ballast layer (19).

Gao and Zhai's track settlement model: Gao and Zhai investigated track settlement by combining the vehicle-track coupling vibration model and the track settlement model. The dynamic response and the irregularities of the track are taken as a feedback to the model. The interaction between vehicle dynamics and dynamic track performance are considered in the study. It is found that the roughness of the surface of the wheel and rail has a strong impact on track settlement behavior (20).

Track vertical deterioration study from BRR (British Rail Research): In the track deterioration study by BRR, the effects of track bed stiffness variation on track geometry deterioration are identified. A number of basic contributors to track geometry deterioration have been determined in order to predict:

- Dynamic forces due to unsprung- mass response to weld dips and the resulting track quality
- Dynamic forces due to unsprung mass response to general track roughness and the resulting track quality and Track quality due to vehicle body response to general track roughness

These three aspects are combined together to calculate the total track SD. However, further equations derived in the track geometry model have not yet been validated. Additionally, the model was only used to analyze limited number of test cases as part of Eurobalt project (21).

Prud'homme studies: The lateral resistance of wooden sleeper track under a moving lateral load was experimentally evaluated. The vertical load remained constant while the lateral load increased after every track loading vehicle (TLV) pass. The first empirical equation for the lateral resistance of track with timber sleepers was developed, and is given as $L_P = 10 + \frac{V}{3}$ Where, L_P…track lateral resistance [kN] and V…vertical axle load [kN] (22).

The Prud'homme limit provides a good guideline to follow the lateral track movement studies, but some important factors, such as curvature and rail thermal load effects, were not considered In the following study, Prud'homme's Equation is improved to reflect the rail temperature, track curvature, track stiffness and rail profile properties as $L_P = \rho\left(10 + \frac{V}{3}\right)$ [23].

Kabo'strack lateral resistance studies: After Prud'homme's study, a three-dimensional FE model was developed to study ballast resistance under vertical and lateral loading against various influencing factors. Four different geometries of ballast shoulder have been analyzed against different vertical loads and friction. The results show that the peak lateral ballast resistance for a single concrete sleeper varies from 5 to 18 kN as the ballast compaction increases. The results also show that the deterioration is not closely related to subgrade stiffness, while the top ballast layer suffers the most strain and is the leading contributor to the settlement (24).

Lateral sliding track resistance study at the University of Southampton: The resistance of the railway track is more complex than the lateral resistance defined by Prud'homme. The sleeper base study is based on an empirical relationship of normal, lateral and moment loads at failure. The maximum bearing capacity of the base resistance can be calculated by:

$V_{max} = N_y S_y (0.5\gamma B - \Delta u) BL$ Where, N_y…analogous to the bearing capacity factor found in the Meyerhof formula, S_y…shape factor from Meyerhof formula, B…foundation width [m], L…foundation length [m], γ…bulk unit weight of ballast [kN/m^3] and u…pore water pressure (25).

Kish, Samavedam et al. investigated the mechanism of track lateral misalignment growth, and developed a model to predict track lateral shift. The parameters used in the track shift analysis are vehicle characteristics, foundation modulus, rail mass, axle vertical and lateral load, rail thermal load, track curvature, and so on (2). Furthermore, the limit in this study varies with the change of vertical load, as shown in Table 2-1-1.

Table 2.1-1 Proposed net axel L/V loading ratio limits (2):

V (kN)	L/V limit	
	L/V=0.28+4.46/V (no alignment defect)	L/V=0.28+3.97/V (with alignment defect)
89	0.50	0.48
133	0.43	0.41
178	0.39	0.38
245	0.36	0.35

Various models of track settlement have been developed to predict the development of vertical track irregularities. However, there have not been many studies about the development of the track lateral misalignment by dynamic load cycles.

Therefore this research tries to fill this gap by investigating an interaction between rail vehicle dynamics and track lateral alignment specifically for Addis Ababa light rail (AALRT) North to South line. The aim of the research is to develop a method for analyzing and predicting railway track lateral deterioration due to rail vehicle dynamics, and determine the triggering or startup limits in terms of track loading and running condition.

2.1.2. Track system models

Track system dynamics has been extensively studied, and various mathematical models have been developed for design and maintenance purposes. Most track models assume that the track system is excited by a single wheel or a single bogie with two wheel-sets. The track system is most commonly modeled either in the frequency or the distance domain. Spatial domain methods use variable frequencies to excite the track at a fixed point along the track, while distance domain methods use variably moving loads applied along the track during a certain time period. Most spatial domain track studies are based on the infinite Euler-Bernoulli and Timoshenko beam models. In general, there are two methods that simulate the vibration behavior of the rail, which are the Finite Element Analysis (FEA) and Vibration Modal method. The vibration modal method effectively reduces the number of Degrees of Freedom (DOF), and hence, the calculation time, while the FEA is better at dealing with nonlinear factors in the track system. Track models are also classified as rails resting on a continuous support or on discrete supports, which are discussed in detail in (27).

2.1.3. Track lateral irregularity studies

Track lateral stability is a key requirement to ensure safety and passenger comfort. Track lateral shift and buckling can cause serious running stability problems or even derailment. Therefore, it is important to identify the mechanism of track lateral movement under dynamic wheel loads. Lateral displacement resistance plays an essential role in stabilizing the track, and it is mainly influenced by the lateral sleeper support, stress free temperature, condition of joints, friction between sleeper and ballast, and the effect of tamping. Unlike the vertical displacement, track lateral displacement is affected by vertical, lateral and longitudinal forces. If the vertical force is high, the resistance between the ballast and the sleeper is high. Therefore, the L/V load ratio is a critical parameter in track lateral movement. The longitudinal force can lead to track uplift or exert a lateral misalignment, shown in Figure 2-1-2. The black line represents the rail, and the orange line shows the longitudinal force and the decomposition of this force along the track and perpendicular to the track (29).

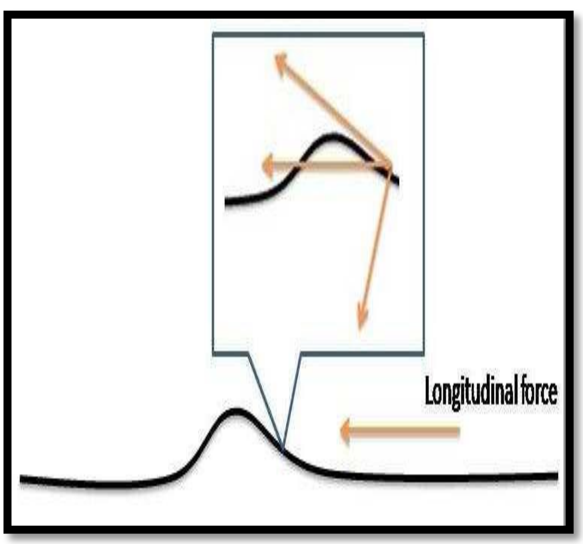

Figure 2.1.2 Initial lateral misalignment effected by longitudinal force (29)

2.1.4. Vehicle-Track Lateral Deterioration Model

In order to obtain the dynamic performance of the rail vehicle accurately, the physical model should be founded based on the geometric model of the rail vehicle. Then its multi-body dynamic model will be set up accurately on the basis of the SIMPACK multi modeling application. For general rail vehicle, it is composed of car body, frame, wheel set, primary suspension and secondary suspension system. The wheel set is connected with the frame by primary suspension, and the car body is connected with frame by secondary suspension. The foreside and rearward bogies of the rail vehicle are the same which are symmetrical to the center of the car body. Only one difference is that the anti-hunting damper is fixed in different place.

2.1.5. Vehicle-track dynamic Interaction model

The characteristics of the wheel – rail contact is of crucial importance for the dynamic interaction between vehicle and track. Therefore, since the 1960s much research has been devoted to the fundamental issues of wheel – rail contact. The wheel – rail contact is, as a rule, very nonlinear. This is true for the so-called contact functions but also for creep forces as functions of creepage and spin (32).

SIMPACK software allows the user to build a dynamic model of any rail vehicle and study the response of the vehicle to real measured track geometry or user specified inputs in the form of track displacements and external force inputs. Rail vehicles can be modeled with simulated instrumentation allowing almost any aspect of the vehicle’s behavior to be studied. This software is used to build dynamic multi-body models of rail vehicles and to capture the forces between the wheels and rails (33).

Chapter three

3.1. Statistical Analysis of Track Quality

This chapter contains a series of statistical analysis studies about the relationship between lateral and vertical irregularities, between track lateral and vertical irregularities and curvature, and about the track deterioration over time. For the first two relationships, it is better to have lots of track data covering long sections of different types of track. For track deterioration over time, it is better to have data covering the same section of track measured at different time intervals. Therefore, track data from the Ethiopian railway corporation has been taken for this research particularly Addis Ababa light rail transit north south line from MESHUALEKIA station to STADIUM station data sets have been used for studying track deterioration over time. This section is chosen as it contains all types of the AALRT track profiles, such as curvatures, switches, super elevation, straight, lines etc. The standard deviation of track alignment low pass filtered below 35m wavelength is generally considered to be a good overall indicator of track quality (34).

The irregularity data filtered at 10m is selected in the statistical analysis for which 10m is the actual length used in AALRT for the purpose of inspection.

3.2. The relationship between track lateral and vertical irregularities

There are many more studies into vertical track deterioration than lateral track deterioration. One of the most important reasons is that the changes in the lateral alignment are slower than the changes in vertical alignment under typical loading cycles (35).

Therefore, maintenance of lateral misalignment is usually considered to be less important. Most track settlement models only include the vertical influence factors and ignore the lateral parameters. The deterioration in the lateral direction is a nonlinear phenomenon because of the highly nonlinear behavior of vehicles in curves or on straight track due to possible hunting behavior, and is related to forces on both vertical and lateral direction. On the contrary, the vertical settlement of track is very much governed by vertical axle load and vehicle speed only.

However, as an indivisible load supporting system, it is possible that the track lateral alignment has an impact on the vertical track settlement behavior. Reduced horizontal residual stresses that confine the ballast layer can decrease the stability of the track (36).

Therefore, it is sensual to analyze the relationship between the lateral and vertical track settlement.

Firstly, a correlation coefficient is used to see if there is a strong linear relationship between track lateral and vertical irregularities. For data sets X = (x1, x2, x3,…., xn) and Y = (y1, y2, y3,…., yn), the level of scatter of the data set around the best-fit line can be measured by the correlation coefficient r, as defined in Equation. The detailed linear regression description is shown in Appendix. The correlation coefficient takes a value between -1 and 1. The data is completely correlated positively when r equals 1 (-1 means correlated negatively), while the data is not linearly related at all when r equals 0. There are three level of correlation: $|r| < 0.4$, shows the data sets are not correlated $0.4 \leq |r| < 0.7$, shows some degree of correlation and$0.7 \leq |r| \leq 1$, indicates a high correlation (15).

$$r = \frac{n\sum x_i y_i - \sum x_i \sum y_i}{\sqrt{n\sum x_i^2 - (\sum x_i)^2}\sqrt{n\sum y_i^2 - (\sum y_i)^2}}$$

Equation 3.2-1

Where, data level X stands for gauge difference or lateral irregularity, data level Y stands for level difference or vertical irregularities, n is the number of data taken and r is correlation coefficient.

Table 3.2-1 Correlation coefficient of track lateral and vertical irregularities

Time of data taken	Correlation coefficient r
June	0.425
October	0.55
January	0.67

The correlations between the vertical and lateral irregularity SD results of track are separately calculated and the coefficients are listed in Table 3.2-1. Generally, the correlation coefficients are bigger than 0.4 which indicates a reasonable relationship between vertical and lateral irregularities, in the sense that decreasing quality in the vertical direction generally coincides with decreasing quality in lateral direction.

3.3. The relationship between track lateral irregularities and curvature

A moving vehicle causes forces between the wheel and rail at the contact patch, which can stress the rail laterally. The lateral force acting on the rails varies with different track curvature, cant and speed. The lateral forces on the high rail of curved track whose radius of curvature is small are much bigger than those on a large curve radius. Track lateral irregularities are created by the forces acting on the track (37).

Therefore, it is necessary to understand the relationship between track lateral irregularities and curvature. It is shown that the lateral forces on the curves are much bigger than on the tangent elements, and the static vertical force is much larger than the dynamic vertical forces.

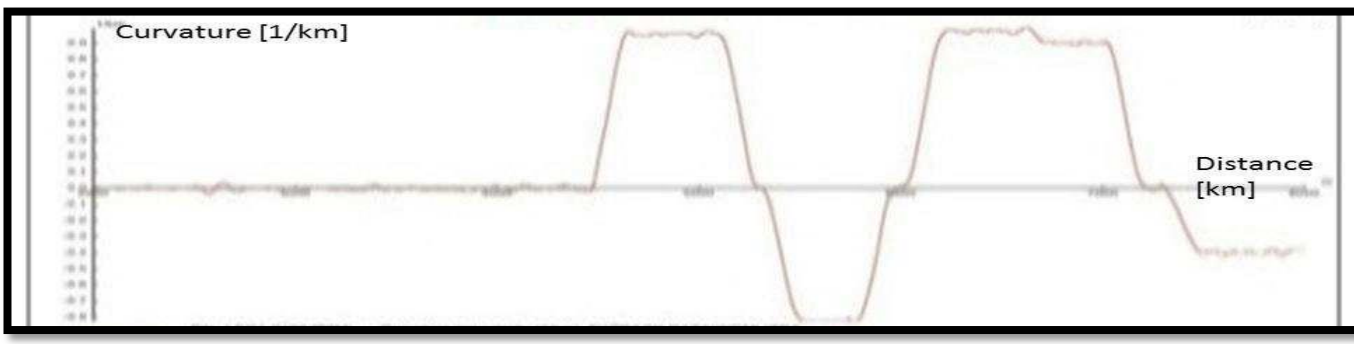

Figure 3.3.1 track curvature vs track length graph (15)

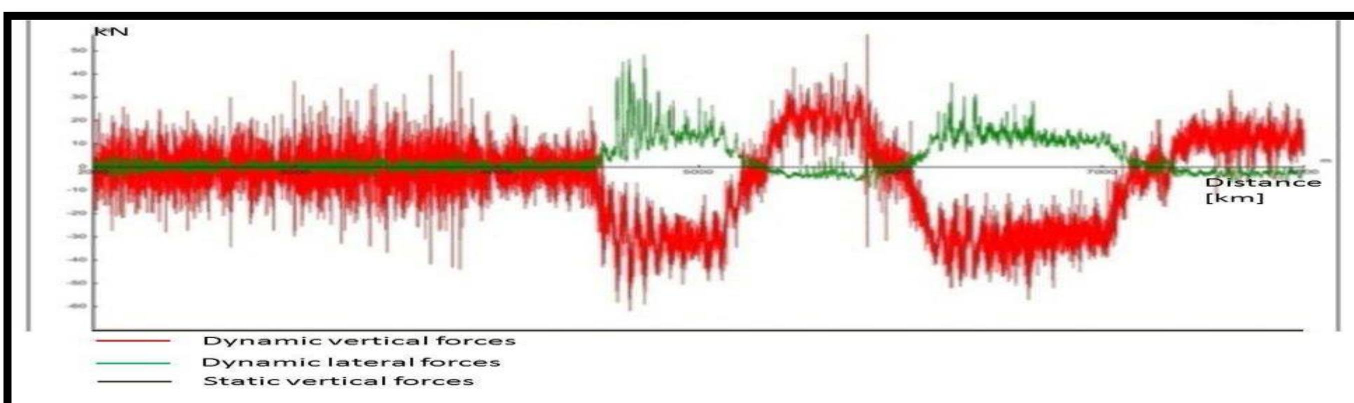

Fig-3.3.2 Track vertical and lateral forces vs track length (15)

3.4. Track lateral deterioration over time

The track data used in this section was recorded by AALRT over a time interval of 2 to 3 months from june 2016 to January 2017 between Studium and Meshualekiya on the North to South Line which has many of the features of AALRT. The total length of this data set is about 780m, containing elements of curved and tangent track.

A model of the growth of track irregularities is presented by Sato, which is influenced by five factors given as:

$$S = 2.09 \times 10^{-3} T^{-0.31} V^{0.98} M^{1.1} L^{0.21} P^{0.26}$$ Equation 3.4-1

Where, S…average irregularity growth rate (mm/100 days) T…traffic tonnage (million tons/year) V…average running speed (km/h) M…structure factor L…influence factor of CWR (Continuous Welded Rail) or jointed rail, 1 for CWR and 10 for jointed P…influence factor for subgrade (1 for good and 10 for bad).

It can be found that the growth of irregularities is almost proportional to the running speed and the repeated loading. Improvement of the track structure can effectively reduce irregularity growth.

The working hours of the AALRT is 16 hours per day and the average practical waiting time at the stations is 15 minutes, so the total number of working hours per year (NWHPY) is calculated as:

$$NWHPY = 16 \times 30 \times 12 + 16 \times 5 = 5760 + 80 = 5840$$

And since waiting time is 15minute, the number of times of tonnage (loading) per hour (NTTPH) is given by:

$$NTTPH = \frac{60}{15} = 4$$

Therefore, a total time of tonnage (loading) of the track per year (TTTTPY) is given by:

$$TTTTPY = 4 \times 5840 = 23360$$

At a time the loading or tonnage is the practical loading on each wheel which is 5332N =5.332ton. so the overall tonnage per year on the track (traffic tonnage in million tons/year) is:

$$Traffic\ tonnage\ in\ \frac{million\ tons}{year} = T = \frac{23360 \times 5.332}{1{,}000{,}000} = 0.125 million\ tons/year$$

$V = 20km/h$ This is the average practical speed as taken from Stadium to Meshualekiya stations in 10 different times.

Structure used here is good which determines the value of the structure factor as M=1 and the influence factor (L) for the rail is 1 since the rail used in AALRT is CWR type. The subgrade used is with good aggregate which implies the value of subgrade influence factor P is 1.

So, S…average irregularity growth rate [mm/100 days] is determined as:

$$S = 2.09 \times 10^{-3} \times 0.125^{-0.31} \times 20^{0.98} \times 2^{1.1} \times 1^{0.21} \times 1^{0.26} = 0.075$$

Therefore the average irregularity growth rate of AALRT is 0.075mm/100 days which is about 2.75mm/year

3.5. Alignment-related track geometry variation

The alignment is one of the major reasons for the lateral vibrations of the railway vehicle. This type of track irregularity can occur during its construction stage, during the maintenance procedures or as a result of the exploitation in the form of a consequence of the accumulated lateral track movements under traffic (34).

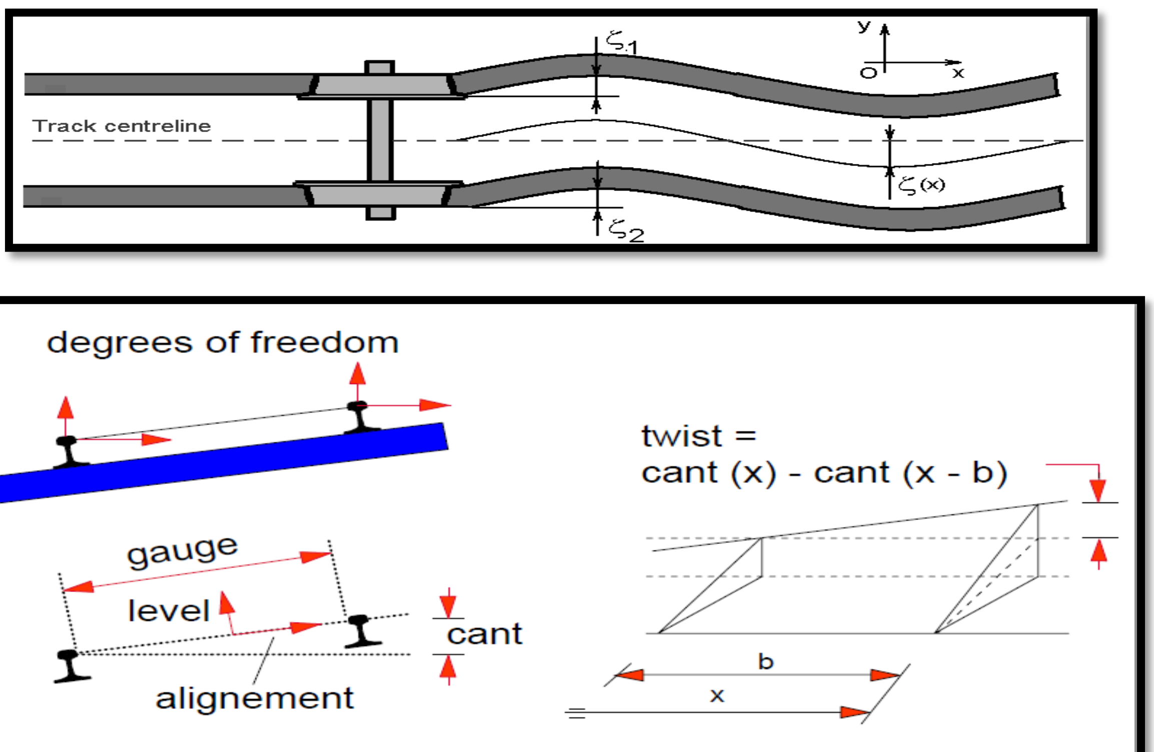

Figure 3.5.1 Track alignment (34)

Track geometry = theoretical value + deviation

Each rail has 2 degrees of freedom, Equivalent level, alignment, gauge and cant (or cross level). An additional one: twist, the difference in cant over a given length.

A simple definition of the alignment is the deviations of the track from its ideal design geometry, characterized by the lateral displacement of each rail, as shown in Fig-3.5.1 The track alignment is the geometrical error, in the traverse direction of the horizontal plane, represented by the difference between a point of the side of the rail, at a height of approximately 15 mm below the running plane, and the ideal mean line of the alignment (34).

3.6. The alignment representation in computational models

The track geometry irregularities represent the primary inputs in the numerical simulations for the dynamics of the railway vehicles. In the review, there are two distinct approaches to include the track irregularities in the computational models. One of the approaches considers the track irregularities as absolute values, defined as distance functions, and obtained by the measurement of the track geometry. Here, the alignment is usually defined on the track centerline, as a mean value of the alignment between left and right rails (38), as in

$$\xi(x) = \frac{\xi_1+\xi_2}{2} \qquad \text{Equation 3.6-1}$$

Another one, frequently used in the studies on the vehicle dynamics, is based on numerous measurements of the track geometry that have shown that the track irregularities represent a stationary stochastic process. In this context, the track irregularities may be introduced in the computational models as stochastic data characterized by the power spectral density. While considering that the alignment $\xi = \xi$ (x), with $0 \leq \xi$ (x) $\leq \xi$ ∞, is a stochastic Gaussian ergotis process, defined by the mean value (39).

3.7. Features of track irregularities

The deviations of the track from the design geometry like the track alignment influences the wheel-rail forces and passenger ride comfort should be limited within a certain interval.

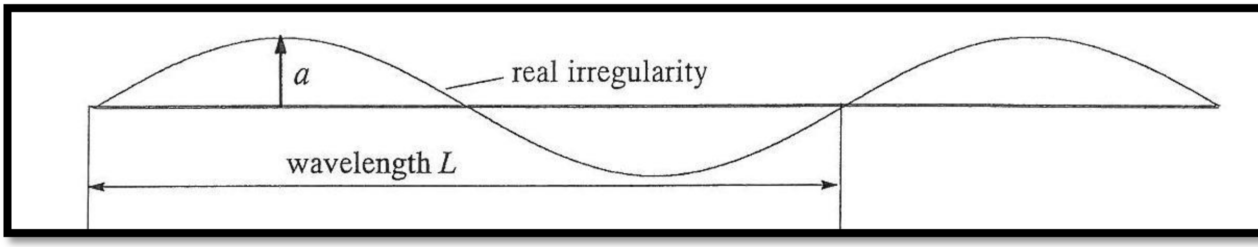

Figure 3.7.1 feature of track irregularity

Definition of Track geometry quality (EN 13848-1:2003+A1:2008) "assessment of excursions from the mean or designed geometrical characteristics of specified parameters in the vertical and lateral planes which give rise to safety concerns or have a correlation with ride quality". Track geometric parameters are Track gauge, longitudinal level, Alignment, Cross level, Twist (40).

3.8. Track irregularities for dynamic analysis

For vehicle dynamic analysis the absolute irregularities as a function of distance have to be known.

But in practice the irregularities are represented as:

Longitudinal level $(z_l + z_r)/2$, $mean\ value\ between\ left\ and\ right\ rail\ in\ vertical\ plane.$

Alignment$(y_l + y_r)/2$, $mean\ value\ between\ left\ and\ right\ rail\ in\ horizontal\ plane$

Gauge$y_l - y_r$, $deviation\ from\ nominal\ track\ gauge$

Cross-level$z_l - z_r$, $deviation\ from\ nominal\ cant$

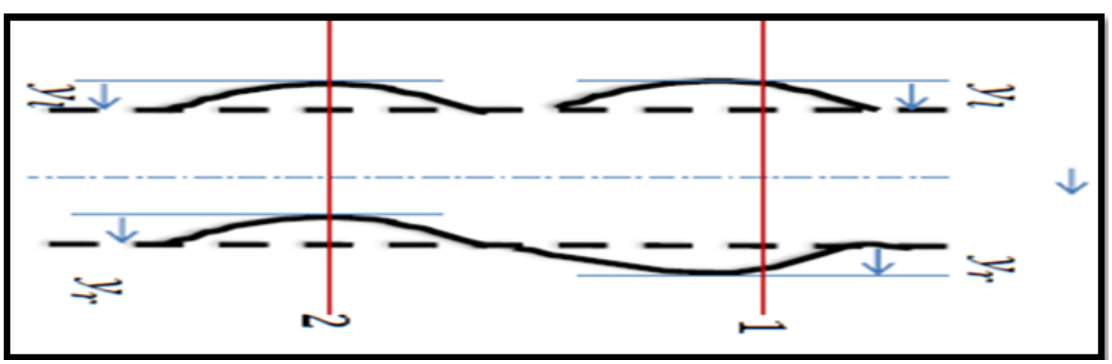

Figure 3.8.1 track irregularity parameters [37]

3.8.1. Gauge and alignment irregularities

Gauge deviation: $y_l - y_r$

Alignment deviation: $(y_l + y_r)/2$

$If\ |y_l| = |y_r| = |y|$

Gauge deviation at 1:

$\leftrightarrow\ (yl - yr) = ((-y) - y) = 2y$

Gauge deviation at 2:

$\leftrightarrow (yl - yr) = (-y) - (-y) = 0$

Alignment deviation at 1:

$\leftrightarrow (yl + yr)/2 = ((-y) + y)/2 = 0$

Alignment deviation at 2:

$\leftrightarrow (yl + yr)/2 = ((-y) + (-y))/2 = -y$

Table 3.8-1: Track length and gauge differences as taken in three different times

DISTANCE	GUAGE AT END OF JUNE	GUAGE AT END OF OCTOBER	GUAGE AT END OF JANUARY
0	0	0	0
10	6	1	1
20	9	10	11
30	9	12	13
40	11	9	13
50	10	12	12
60	8	10	10
70	10	11	10
80	10	4	3
90	5	-1	3
100	3	-1	3
110	3	0	0
120	0	1	0
130	0	1	0
140	0	2	1

DISTANCE	GUAGE AT END OF JUNE	GUAGE AT END OF OCTOBER	GUAGE AT END OF JANUARY
150	2	-2	2
160	-1	0	0
170	0	-2	0
180	-2	-2	-1
190	-1	-2	-1
200	-1	0	0
210	0	0	0
220	0	0	0
230	0	0	-1
240	0	0	0
250	0	0	-1
260	0	1	0
270	1	1	1
280	1	1	0
290	-1	-1	-2
300	2	2	2
310	1	2	2
320	-1	-1	-2
330	-1	0	0
340	0	-1	0
350	-1	1	-1
360	0	2	0
370	-1	0	-1
380	0	0	0
390	-1	-1	-2
400	1	2	1

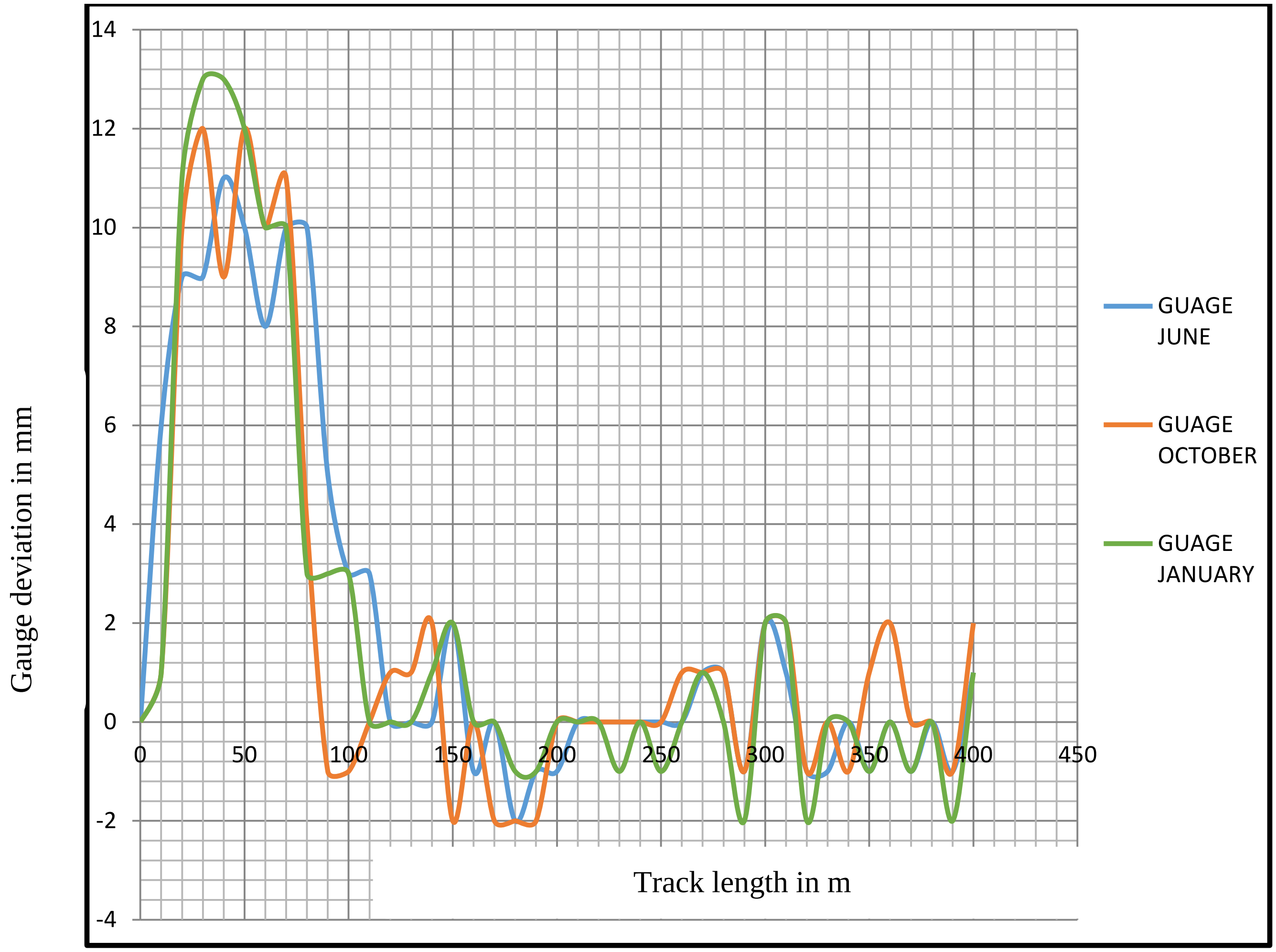

Figure 3.8.2 Relation between track length and gauge deviations of measured data

As seen from figure 3.8.2, the value of gage deviation bigger too much around 25 m from stadium and this is due to switches and turnouts where the track starts to be curved and separation of the track from Ayat line to Kality line. Based on this graph the values of track gauge deviation are generally bigger on curved sections than the straight sections.

Table 3.8-2: Statistical interpretations for track lateral irregularities collected in June 2016

Parameter	Track length	Irregularity (gauge difference) error
Sum	8200	8.1
Mean	200	0.173
Maximum	400	1.1

Minimum	0	-0.2
Standard deviation	13.04536713	

Table 3.8-3: Statistical interpretations for track lateral irregularities collected in October 2016

Parameter	Track length	Irregularity (gauge difference) error
Sum	8200	7.1
Mean	200	0.185
Maximum	400	1.2
Minimum	0	-0.2
Standard deviation	13.05067786	

Table 3.8-4: Statistical interpretations for track lateral irregularities collected in January 2017

Parameter	Track length	Irregularity (gauge difference) error
Sum	8200	7.6
Mean	200	0.195
Maximum	400	1.3
Minimum	0	-0.2
Standard deviation	13.05493391	

From these three tables it is clearly observed that lateral irregularity or gauge difference is increasing with time till the limiting value (outer end of flange contact) is attained where the limiting value for allowable gauge error is -3mm and 5mm.

Table 3.8-5: Track length and vertical elevation differences as taken in three different times

DISTANCE	VERTICAL ELEVATION AT END OF JUNE	VERTICAL ELEVATION AT END OF OCTOBER	VERTICAL ELEVATION AT END OF JANUARY
0	-1.3	-1.3	-1.3

DISTANCE	VERTICAL ELEVATION AT END OF JUNE	VERTICAL ELEVATION AT END OF OCTOBER	VERTICAL ELEVATION AT END OF JANUARY
10	-1.3	-0.3	0.7
20	3.63798E-11	-1	3.64E-11
30	1	-1	-1
40	3.63798E-11	-1	1
50	-1	-4.18E-10	-1
60	-1	-1	3.64E-11
70	-5	-7	-6
80	1.9	-13.1	-25.1
90	-3.1	-13.1	-16.1
100	0	-5	-3
110	-5	0	-3
120	-1	1	-1
130	0	2	-1
140	2	2	1
150	1	2	-1
160	1	-4	-3
170	-2	1	-4
180	-2	1	-4
190	0.2	-0.8	-6.8
200	0.2	-0.8	-0.8
210	1.81899E-10	-3	-4
220	1.81899E-10	3	-4
230	-2	2	-5
240	-2	-1	-3
250	-3	-1	-2
260	-6	-2	-2

DISTANCE	VERTICAL ELEVATION AT END OF JUNE	VERTICAL ELEVATION AT END OF OCTOBER	VERTICAL ELEVATION AT END OF JANUARY
270	1.81899E-10	-1	-1
280	-1	1	-3
290	-4	-4	-4
300	-2.72848E-10	-2	-2
310	1.81899E-10	1	9
320	1.81899E-10	2	1.82E-10
330	-3.9	-2.9	-22.9
340	0.2	0.2	17.2
350	1.2	2.2	1.2
360	-1	3	-1
370	-0.6	13.4	-1.6
380	0.3	1.3	-0.7
390	-0.7	0.3	-1.7
400	2	1	-5.46E-11

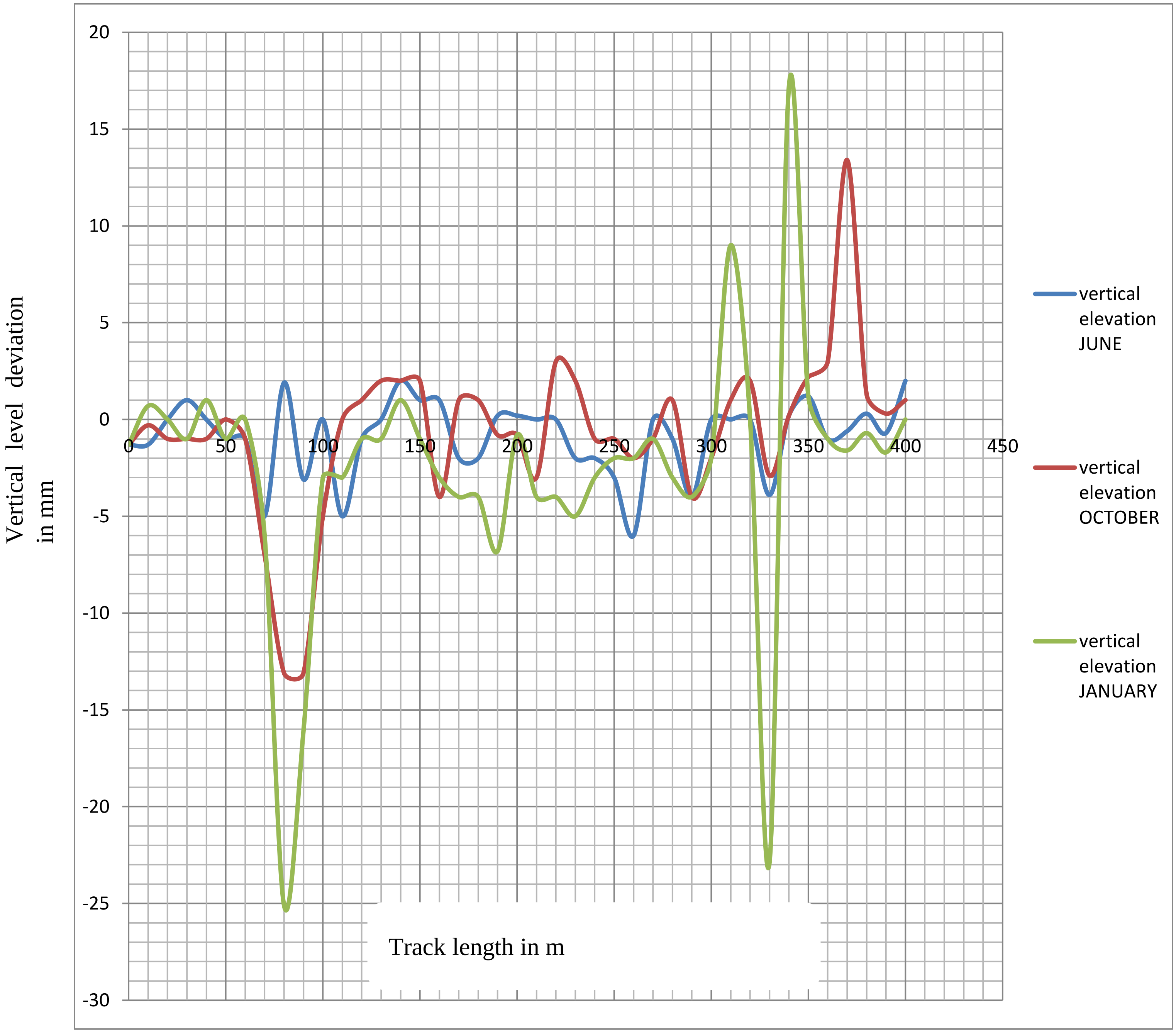

Figure 3.8.3 Relation between track length and vertical level deviations of measured data

Figure 3.8.3 indicates some maximum values at random sections of the track and these sections are locations of track where the ballast and sleepers are fallen from their original or proper places indicating that the ballast and sleepers need to be inspected continuously to ensure proper track - vehicle vertical alignment.

Table 3.8-6: Statistical interpretations for track vertical irregularities collected in June 2016

Parameter	Track length	vertical irregularities (level difference) error
Sum	8200	-3.59
Mean	200	0.088
Maximum	400	0.2
Minimum	0	-0.6
Standard deviation	13.14724815	

Table 3.8-7: Statistical interpretations for track vertical irregularities as collected in October 2016

Parameter	Track length	vertical irregularities (level difference) error
Sum	8200	-2.69
Mean	200	-0.066
Maximum	400	1.34
Minimum	0	-1.31
Standard deviation	13.15314164	

Table 3.8-8: Statistical interpretations for track vertical irregularities collected in January 2017

Parameter	Track length	vertical irregularities (level difference) error
Sum	8200	-10.59
Mean	200	-0.258
Maximum	400	1.72
Minimum	0	-2.51
Standard deviation	13.2268766	

The three statistic tables indicate that the vertical irregularities are increasing as operational time proceeds in the same way for lateral irregularities and the limiting values of vertical level difference error is ±6mm.

3.8.2. Track quality

Track geometry quality is related to vehicle running dynamics, Safety, Running stability and Comfort and is also related to track maintenance, Dynamic track forces and Track deterioration, including track components, ballast, sub ballast, soil and bridges. Track geometry quality is a determining factor for setting train speed. Good Track geometry quality implies economical & safe well for passengers and goods (41).

3.8.3. The numerical simulation of track irregularities

Track irregularity is a non-deterministic excitation on the rail vehicle, which includes vertical, alignment, cross-level, and gauge irregularity. Critical speeds are affected by the vertical and cross-level irregularities mainly. The vertical irregularity Sv (ω) and alignment irregularity Sa (ω) are:

$$\boldsymbol{S_v(\omega) = \frac{KA_v{\omega_c}^2 v}{\omega^2(\omega^2+{\omega_c}^2)}} \qquad \text{Equation 3.8-1}$$

$$\boldsymbol{S_a(\omega) = \frac{KA_a{\omega_c}^2 v}{\omega^2(\omega^2+{\omega_c}^2)}} \qquad \text{Equation 3.8-2}$$

Where, $S_v(\omega)$ and $S_a(\omega)$ are vertical and alignment irregularity power spectral densities, $cm^2.m$ /rad, ω and ω_c are frequency and cut-off frequency separately, A_a and A_v are parameters which are taken as irregularity amplitude, v is the speed of vehicle, k is factor, and generally it is taken to be 0.25 (42).

Based on the above theory and the track spectrum formulas, the program is designed using SIMPACK, and the vertical and alignment irregularities amplitude waveform in time domain were simulated.

3.8.4. Track lateral shift model

A Finite Element (FE) model was selected to investigate the non-linear lateral behavior of the track. Although it is widely used in engineering, the drawback is that it can be time consuming to model a complete track system due to the large number of elements and degrees of freedom required. Track lateral settlement is caused by multiple passages of vehicles that would take an extremely long time to calculate using FE modeling (15).

In the single sleeper lateral shift analysis, the bending behavior of the sleeper is simplified to have a linear relationship with the rail deflection. This can lead to an inaccurate analysis result, thus it is necessary to model the rail bending for a certain length of the track. In the track lateral shift analysis, the nonlinear factors are inevitable consequently an FE model is best suited to describe the behavior of the rail, sleepers and track bed.

The rails are divided by the length of the sleeper distance to create the discrete rail elements. When there are N nodes on the rail, there will be N sleepers and N-1 rail elements. For the lateral model only the track behavior in the lateral direction is considered, so every rail node has 2 DOF which means that the total rail DOF is 2N.

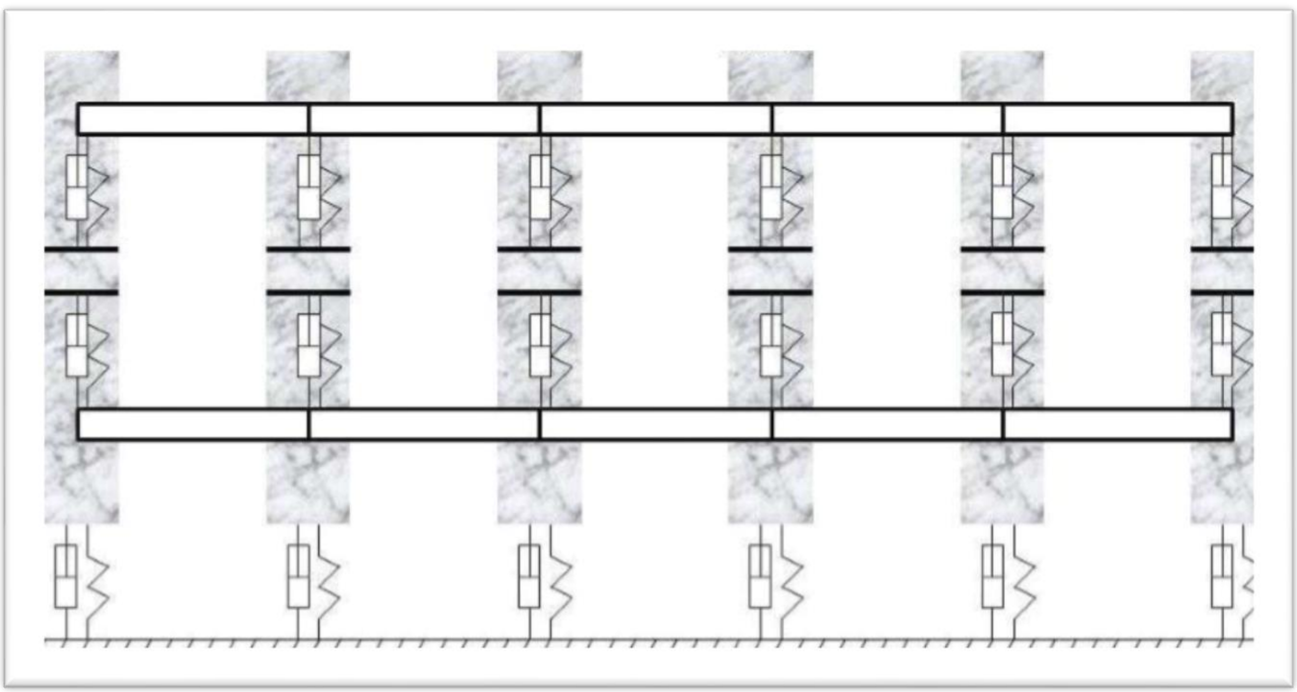

Figure 3.8.4 Track discretization (15)

The equations of motion of the track lateral shift model are defined in Equation below based on the principle of total potential energy of a dynamic system (33).

$$[M]\{\ddot{q}\} + [C]\{\dot{q}\} + [K]\{q\} = \{F(t)\}$$ Equation 3.8-3

The formulation of the model is made in two steps. After the FE rail model is built, the MBS model of the discrete sleeper and continuous track bed support will be added into the model.

3.8.5. FE rail model

Assuming on the i^{th} element, moment, M_i, M_{i+1} and lateral forces, F_i, F_{i+1} are applied respectively on node i and i+1as shown in the figure below. The rail element displacement vector is given as:

$$\{u_i\}^e = \begin{Bmatrix} \{u_1\}^e \\ \{u_2\}^e \end{Bmatrix} = \begin{bmatrix} u_i \\ \theta_i \\ u_{i+1} \\ \theta_{i+1} \end{bmatrix}$$

Equation 3.8-4

Where, u_i, u_{i+1} are displacements of each node and θ_i, θ_{i+1} are rolling angels of each element.

There are several different methods used to obtain the stiffness matrix of the rail element: Hermite interpolation (23), direct stiffness method and principle of virtual work (24). The Hermite interpolation method is selected in this study due to its convenience in finding out the complete mass, damping and stiffness matrix. Therefore, the displacement of the rail element on any point is:

$$u_{ri}(x) = [N]\{u_i\}^e$$

Equation 3.8-5

$$[N] = [N_1, N_2, N_3, N_4]$$

Equation 3.8-6

$$\begin{cases} N_1 = 1 - 3\left(\frac{x}{L}\right)^2 + 2\left(\frac{x}{L}\right)^3 \\ N_2 = x\left[1 - 2\left(\frac{x}{L}\right) + 2\left(\frac{x}{L}\right)^2\right] \\ N_3 = \left(\frac{x}{L}\right)^2\left(3 - 2\frac{x}{L}\right) \\ N_4 = x\left[\left(\frac{x}{L}\right)^2 - \frac{x}{L}\right] \end{cases}$$

Equation 3.8-7

The vibration kinetic energy and bending strain energy of the rail element are respectively:

$$T_i = \frac{1}{2}\int_0^L m_r \dot{u}_i^2(x)dx = \frac{1}{2}\{\dot{u}_i\}^{eT}\left[\int_0^L m_r[N]^T[N]dx\right]\{\dot{u}_i\}^e$$

Equation 3.8-8

$$U_i = \frac{1}{2}\int_0^L EI\left(\frac{d^2u_i(x)}{dx^2}\right)^2 dx = \frac{1}{2}\{u_i\}^{eT}\left[\int_0^L EI\left(\frac{d^2N}{dx^2}\right)^T\left(\frac{d^2N}{dx^2}\right)dx\right]\{u_i\}^e$$

Equation 3.8-9

Substituting the equation3 into the Equation 5 and integrating, the mass matrix of the rail element is established as:

$$[m] = \frac{m_r L}{420}\begin{bmatrix} 156 & 22L & 54L & -13L \\ 22L & 4L^2 & 13L & -3L^2 \\ 54L & 13L & 156 & -22L \\ -13L & -3L^2 & -22L & 4L^2 \end{bmatrix}$$ Equation 3.8-10

Substituting Equation 3 into Equation 5 and integrating, the stiffness matrix of the rail element is:

$$[k] = \frac{EI}{L^3}\begin{bmatrix} 12 & 6L & -12 & 6L \\ 6L & 4L^2 & -6L & 2L^2 \\ -12 & -6L & 12 & -6L \\ 6L & 2L^2 & -6L & 4L^2 \end{bmatrix}$$ Equation 3.8-11

Assuming there is a concentrated load P(t) on x=l, then the virtual work done by the force is:

$$\delta W_i = P\delta u_i(l) = P\{\delta u_i\}^{eT}[N]_{x=l}$$ Equation 3.8-12

So, the force on the element is expressed as:

$$\{F_i\}^e = [F_i \quad M_i \quad F_{i+1} \quad M_{i+1}] = P[N]_x^T = [PN_1 \quad PN_2 \quad PN_3 \quad PN_4]_{x=l}^T$$ Equation 3.8-13

3.8.6. Track lateral model development

According to the track lateral model shown in Figure 4-14, the unknown lateral displacement vector and the input force matrix of the two rails nodes and the sleepers are written as:

$$\{F\} = \begin{bmatrix} F_{11} \\ M_{11} \\ F_{12} \\ M_{12} \\ \vdots \\ F_{1N} \\ M_{1N} \\ F_{21} \\ M_{21} \\ F_{22} \\ M_{22} \\ \vdots \\ F_{2N} \\ M_{2N} \\ F_{s1} \\ F_{s2} \\ \vdots \\ F_{sN} \end{bmatrix} \qquad \{u\} = \begin{bmatrix} u_{11} \\ \theta_{11} \\ u_{12} \\ \theta_{12} \\ \vdots \\ u_{1N} \\ \theta_{1N} \\ u_{21} \\ \theta_{21} \\ u_{22} \\ \theta_{22} \\ \vdots \\ u_{2N} \\ \theta_{2N} \\ u_{s1} \\ u_{s2} \\ \vdots \\ u_{sN} \end{bmatrix}$$ Equation 3.8-14

The same principle and method are used to build the complete track lateral shift model with N sleepers. The vibration kinetic energy, bending strain energy and the virtual work of the whole track system can be written as:

$$T = \frac{1}{2}\sum_{i=1}^{N-1}\{\dot{u}_{1i}\}^{eT}[m]^{e}\{\dot{u}_{1i}\}^{e} + \frac{1}{2}\sum_{i=1}^{N-1}\{\dot{u}_{2i}\}^{eT}[m]^{e}\{\dot{u}_{2i}\}^{e} + \frac{1}{2}\sum_{i=1}^{N} m_s \dot{u}_{si}^2$$

Equation 3.8-15

$$U = \frac{1}{2}\sum_{i=1}^{N-1}\{u_{1i}\}^{eT}[k]^{e}\{u_{1i}\}^{e} + \frac{1}{2}\sum_{i=1}^{N-1}\{u_{2i}\}^{eT}[k]^{e}\{u_{2i}\}^{e} + \frac{1}{2}k_r\sum_{i=1}^{N}(u_{1i}-u_{si})^2 + \frac{1}{2}k_r\sum_{i=1}^{N}(u_{2i}-u_{si})^2 + \frac{1}{2}k_s\sum_{i=1}^{N}u_{si}^2$$

Equation 3.8-16

$$\delta W = c_r\sum_{i=1}^{N}(2\dot{u}_{si}-\dot{u}_{1i}-\dot{u}_{2i})(2\delta u_{si}-\delta u_{1i}-\delta u_{2i}) + c_s\sum_{i=1}^{N}\dot{u}_{si}\delta u_{si} + F_1(t)\{\delta u_{1i}\}[N]_{x=l}$$

Equation 3.8-17

3.9. Technical Parameters of Dynamic wheel rail interaction model for AALRT

This research thesis is used to simulate Addis Ababa light-railway transit project rail dynamic analysis due to the impact of flat wheel. For this simulation, LRT tramcar is shown on the figure 3.7. This tramcar type is 6-axle double-articulated 70% low-floor Light Rail tramcar and is formed with three modules, which are Mc, T and Mc. Under the Mc module of the tramcar body a bi-axial power bogie is installed, and a bi-axial driven bogie with independent wheel is installed under the T module [17].

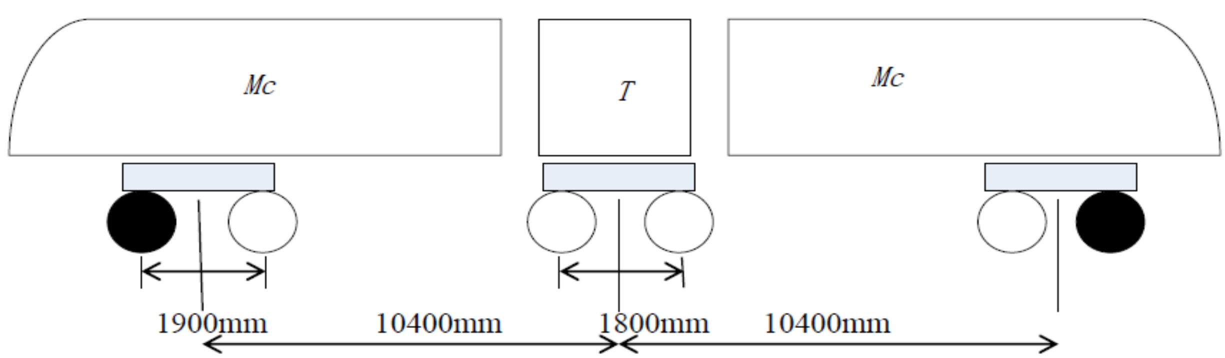

Figure 3.9.1 Tram car lay out with its respective length (17)

According to the data recorded in (17), the following technical parameters are given in the table.

Table: Vehicle Technical parameters used by AALRT and in modeling for this paper

No.	Parameters	Values	Units
1	The speed of the vehicle	Highest speed – 80 but 20 is taken which is the maximum actual running speed in between Stadium and Meshualekia stations.	km/h
2	Tram car length	28400	mm
3	Weight of tram car	43	t
4	Track gauge	1435	mm
5	Distance between two sleeper pads	0.658 for mainlines and 0.625 for elevated	m
6	Rail standard in AA-LRT	TB10082-2005 (50kg/m)	kg/m
7	Length of the rail	25	m
8	Height of rail	153	mm
9	Top width of the rail	65	mm
10	Foot width of the rail	134	mm
11	Rib thickness	15.5	mm
12	Cross sectional area of rail	64.16	cm^2
13	Young modulus of rail	210.8	Gpa
14	Cross sectional Mass of rail	60	kg/m
15	The pads	rubber cushion (polyethylene)	-
16	Concrete sleeper mass	308	kg

17	Wheel diameter	660 for motor wheel, 600 for driven wheel	mm
18	Sleeper top width	220	mm
19	Sleeper bottom width	250	mm
20	Sleeper height	208	mm
21	Sleeper length	2200	mm
22	Sleeper spacing	0.6	m
23	Rail Section moment of area about vertical axis (I_{yy})	5.123×10^{-6}	m^4
24	Rail Section moment of area about horizontal axis (I_{zz})	3.038×10^{-5}	m^4
25	Rail pad length	180	mm
26	Rail pad width	150	mm
27	Rail pad thickness	7.5	mm
28	Load on each wheel	5,332	N
29	Sleeper-ballast lateral stiffness	40,000	KN/m
30	Sleeper-ballast vertical stiffness	90,000	KN/m
31	Sleeper-ballast lateral damping	2.5×10^4	N.s/m
32	Sleeper-ballast vertical damping	8×10^4	N.s/m
33	Rail pad lateral stiffness	39,800	KN/m

34	Rail pad vertical stiffness	63,000	KN/m
35	Rail pad lateral damping	$3x10^4$	N.s/m
36	Rail pad vertical damping	$4x10^4$	N.s/m

Based on the above equations and the data taken from AALRT document, the mass matrix [M] is calculated using MATLAB and given below where, and L are rail mass per m and L is tack length while A is four by four matrix respectively.

>> mr=60; L=25;

>> A=[156,22*L,54*L,-13*L;22*L,4*L^2,13*L,-13*L^2;54*L,13*L,156,-22*L;-13*L,-3*L^2,-22*L,4*L^2;]

A =

$$\begin{matrix} 156 & 550 & 1350 & -325 \\ 550 & 2500 & 325 & -8125 \\ 1350 & 325 & 156 & -550 \\ -325 & -1875 & -550 & 2500 \end{matrix}$$

>> M=((mr*l)/420)*A

[M] = 1.0e+04 *

0.0557 0.1964 0.4821 -0.1161

0.1964 0.8929 0.1161 -2.9018

0.4821 0.1161 0.0557 -0.1964

-0.1161 -0.6696 -0.1964 0.8929

And the stiffness matrix K_v is calculated using MATLAB and to give results as below.

Vertical stiffness matrix is evaluated below where, E, L, I and B are young's modulus, track length, rail section moment of are and four by four matrixes respectively.

>> E=2.08*10^11;L=25;Iyy=5.123*10^-6;

>> B =[12,6*L,-12,6*L;6*L,4*L^2,-6*L,2*L^2;-12,-6*L,12,-6*L;6*L,2*L^2,-6*L,4*L^2;]

K_v=((E*Iyy)/L^3)*[12,6*L,-12,6*L;6*L,4*L^2,-6*L,2*L^2;-12,-6*L,12,-6*L;6*L,2*L^2,-6*L,4*L^2;]

[K_v]= 1.0e+05 *

0.0082 0.1023 -0.0082 0.1023

0.1023	1.7049	-0.1023	0.8525
-0.0082	-0.1023	0.0082	-0.1023
0.1023	0.8525	-0.1023	1.7049

Similarly, lateral stiffness matrix is:

```
>> E=2.08*10^11;L=25;Iyy=3.038*10^-5;
>> KL=((E*Iyy)/L^3)*[12,6*L,-12,6*L;6*L,4*L^2,-6*L,2*L^2;-12,-6*L,12,-6*L;6*L,2*L^2,-6*L,4*L^2;]
```

$[K_L]$=

1.0e+06 *

0.0049	0.0607	-0.0049	0.0607
0.0607	1.0110	-0.0607	0.5055
-0.0049	-0.0607	0.0049	-0.0607
0.0607	0.5055	-0.0607	1.0110

Now the equation of motion is used to show the relationship between both vertical and lateral forces with time taken to cover a 25 m (q=25m) rail as follows.

$$[M]\{\ddot{q}\} + [C]\{\dot{q}\} + [K]\{q\} = \{F(t)\}$$

$$\dot{q} = \frac{dq}{dt} \rightarrow \dot{q}dt = dq \rightarrow \int_0^t \dot{q}dt = \int_0^{25} dq \rightarrow \dot{q} = \frac{25}{t} \text{ and } q = \int \frac{25}{t} \rightarrow q = \frac{-25}{t}$$

Similarly $\ddot{q} = -\frac{25}{t^2}$

So vertical loading on the rails is given by:

$$F_v(t) = [M]\left\{-\frac{25}{t^2}\right\} + C_v\left\{\frac{25}{t}\right\} + [K_v]\{\frac{-25}{t}\}$$

Up on substitution the values of terms respectively it gives:

$$F_v(t) = 25e+04 \times \begin{bmatrix} 0.0557 & 0.1964 & 0.4821 & -0.1161 \\ 0.1964 & 0.8929 & 0.1161 & 0.1161 \\ 0.4821 & 0.1161 & 0.0557 & -0.1964 \\ -0.1161 & -0.6696 & -0.1964 & 0.8929 \end{bmatrix} \times \left\{-\frac{1}{t^2}\right\} + 75 \times 10^4 \times \left\{\frac{1}{t}\right\} +$$

$$25e+05\begin{bmatrix} 0.0082 & 0.1023 & -0.0082 & 0.1023 \\ 0.1023 & 1.7049 & -0.1023 & 0.8525 \\ -0.0082 & -0.1023 & 0.0082 & -0.1023 \\ 0.1023 & 0.8525 & -0.1023 & 1.7049 \end{bmatrix}\{\frac{-1}{t}\}$$

And lateral loading on the rails is given by:

$$F_L(t) = [M]\left\{-\frac{25}{t^2}\right\} + C_L\left\{\frac{25}{t}\right\} + [K_L]\{\frac{-25}{t}\}$$

$$F_L(t) = 25e+04 \times \begin{bmatrix} 0.0557 & 0.1964 & 0.4821 & -0.1161 \\ 0.1964 & 0.8929 & 0.1161 & 0.1161 \\ 0.4821 & 0.1161 & 0.0557 & -0.1964 \\ -0.1161 & -0.6696 & -0.1964 & 0.8929 \end{bmatrix} \times \left\{-\frac{1}{t^2}\right\} + 100\times 10^4$$

$$\times\left\{\frac{1}{t}\right\}+$$

$$25e+06\begin{bmatrix} 0.0049 & 0.0607 & -0.0049 & 0.0607 \\ 0.0607 & 1.0110 & -0.0607 & 0.5055 \\ -0.0049 & -0.0607 & 0.0049 & -0.0607 \\ 0.0607 & 0.5055 & -0.0607 & 1.0110 \end{bmatrix}\{\frac{-1}{t}\}$$

When similar 5.49167N KN loads are applied on both right and left rails, moving from the first node to the last at a speed of 20Km/h (5.5/s) which is taken during the peak operation hours. During taking speeds of trains the values recorded are given below in table format.

Table 3.9-1: Data taken during peak operation hours of AALRT

Parameter	Value	Unit
Track length from Stadium to Mesualekiya	800	Meter
Running time	190	Second
Maximum speed	5.5 (20)	m/s (Km/h)
Minimum speed	3.76 (14)	m/s (Km/h)
Average speed	4.211 (15.2)	m/s (Km/h)
Maximum capacity	9.5	Passengers/m^2

In order to get more accurate simulation results, a 3D model integrated drivetrain substructure was established in commercial package SIMPACK, which is widely used to General Mechanical System Analysis & Design. SIMPACK is a general MBD tool that used to model a rail vehicle as a generic mechanism, running on rails. In SIMPACK Kinematics and dynamics are fully nonlinear and all degrees of freedom are available, like in reality, Gravity (crests, dips) are fully considered, Centrifugal forces (curving) and gyroscopic moments results from actual movements, Vehicle is actually slowing down from energy dissipation (rail-wheel contact, dampers, friction), Derailment and post-derailment simulation possible in this MBD application tool.

Generally, trains often run under various speed, for example, traction and braking. Conditions in traction and braking are severe for wheel set vibration, so wheel set bearing vibration feature should be researched under traction and braking conditions.

All load data are used based on AA-LRT (43). Vertically downward load is sum of all vertical loads including 3% allowance of maximum axle load. The overall load is the sum of the total tram weight and carrying capacity of the vehicle. The overall load is classified to each axle of the vehicle then the axle load is classified to each wheel vehicle. Carrying capacity of vehicle has been calculated by taking an average of 60kg for each person and the total rate of passenger inside of the tramcar is 317 for the maximum design capacity of the tram. But practically the number of persons/m^2 is about 9.5 during the peak hours of operation which implies about 365 passengers during peak operation hours (7:30 AM to 3:00AM and 5:30PM to 7:30PM as it is checked from Monday to Friday).

Table 3.9-2: Tram car capacity

Item No.	Number of passengers (persons)	Seated	Standing	Total
1	Seats (AW_1)	65	0	65
2	Seating capacity (AW_2) (standing :6 persons/m^2)	65	189	254
3	Over loading capacity (AW_3) (standing :8 persons/m^2)	65	252	317

Table 3.9-3: Tram car weight

Item No.	Loads	Carboy weight	Passenger weight	Total weight
1	Empty vehicle (t)	44	0	44
2	Seating capacity (t)	44	15.24	59.24
3	Over loading capacity (t)	44	19.02	63.02
4	Axel load (t)	≤ 11 (1+3%)		
5	Axel number	6		

The total vertical load is calculated as follows:

A. $Tram\ car\ weight\ =\ 44\ ton$

$The\ load\ apply\ on\ each\ axle\ =\ 44/6 = 7.333\ ton \times 1000\ =\ 7333.3N$

$The\ load\ applied\ on\ each\ wheel\ =\ 7.333\ ton\ /2 = 3.667\ ton \times 1000\ =\ 3666.7\ N$

B. $Carrying\ Capacity\ =\ 60kg/person\ \times 317\ person\ =$ $19020N\ for\ design\ overloading\ case.$

But practically, AALRT is operating with 9.5 passengers/m^2 which gives$Practical\ Carrying\ Capacity = \frac{60kg}{person} \times 365 \frac{person}{m^2} = 21900N.$

C.$Over\ all\ capacity\ =\ Tram\ car\ weight\ on\ each\ wheel\ +\ Carrying\ Capacity =$ $21900N + 44000N$

$= 65900N.$

This implies that the practical axel loading value is:

$\frac{65900N}{6} = 10983.333N$ And loading values on the each wheel is $\frac{63980}{12} = 5491.67N$

D. $Maximum\ Axle\ load\ =\ 11{,}000\ kg\ \times 9.81m/m^2 = 107{,}910N$

E. $The\ total\ vertical\ load\ =\ maximum\ Axle\ load\ + 3\%\ maximum\ Axle\ load$

$=\ 111147.3N$

f. $The\ load\ on\ each\ wheel\ =\ 55573.63$N This is a design value.

Note: The maximum practically applied axle or wheel load (10983.333N or 5491.67N) is chosen for the analysis which means the maximum parameter is used to perform the analysis. In order to attain the accurate analysis for any application, the support and the load are defined. The place where the sleepers contact the rail is considered as fixed support.

3.10. SIMPACK modeling

In order to perform the computer simulations, a suitable model have to be created first. This could be done using different Multi Body Simulation software. In this project, one of the most well-known software accepted by industrial and academic communities called Multi Body Simulation (MBS) software SIMPACK9.8.2 rail module is used.

The MBS software SIMPACK v9.8.2 allows the user to create a railway model with different levels of complexities including large number of degrees-of-freedom, different types of suspension elements, several contact models, wheel and rail profiles, and so on. SIMPACK rail module is known as one of the best computer simulation environments which together with the possibility of importing measurement data provides a relatively cheap and reliable package for design and verification of new or modifying the existing rail models by the industry.

3.11. Rail - Wheel Pair

The first step to create a SIMPACK rail model is the specification of the number of wheel sets composing the railway model. By doing this, the user is asked to fulfill the panel Rail-Wheel Pair in which the contact between rail and wheel is defined for each wheel set. This panel is divided into five tabs by which properties such as rail and wheel profile, material parameters or friction coefficient have to be defined. In the "Wheel" tab, the main aspects asked by the software are the wheel profile (S1002 used in this project) as well as the nominal wheel radius and lateral distance between wheels. Concerning the Rail tab, the type of rail profile (UIC 60 for this project) and the rail cant (inward inclination of the rail with respect to the vertical plane) are asked. In Contact, Normal Force tab, the user is asked to define the theory used to calculate the normal contact forces. For this project the contact type Hertzian is selected as recommended by SIMPACK. Finally in Tangential Forces tab, the type of theory by which the tangential contact forces are computed is defined. Even though SIMPACK provides several options, for this project the FASTSIM algorithm has been used for being a simplified version of the nonlinear contact. It calculates the contact forces in different directions in a fast and reliable way which is suitable when performing optimization routines. Rail-Wheel pair panel is dedicated to define the characteristics of the rail-wheel contact.

Table 3.11-1 Wheel and rail properties

Wheel Profile	**S1002**
Nominal radius	0.33m
Rail Profile	UIC60
Rail cant	1:40
Young modulus (GPa)	210
Poisson number	0.25
Kinematic coefficient of friction	0.45

Every other aspect considered in this panel was defined as in the configuration recommended by SIMPACK.

Table 3.11-2 Track properties

Curved section 1 from stadium	Length in m	30
	Radius in m	300
	Super Elevation in mm	0
Curved section 2	Length in m	95
	Radius in m	50
	Super Elevation in mm	40
Curved section 3	Length in m	100
	Radius in m	55
	Super Elevation in mm	40
	Length in m	175

Straight	Radius in m	2000
	Super Elevation in mm	0
Total track length in m		400

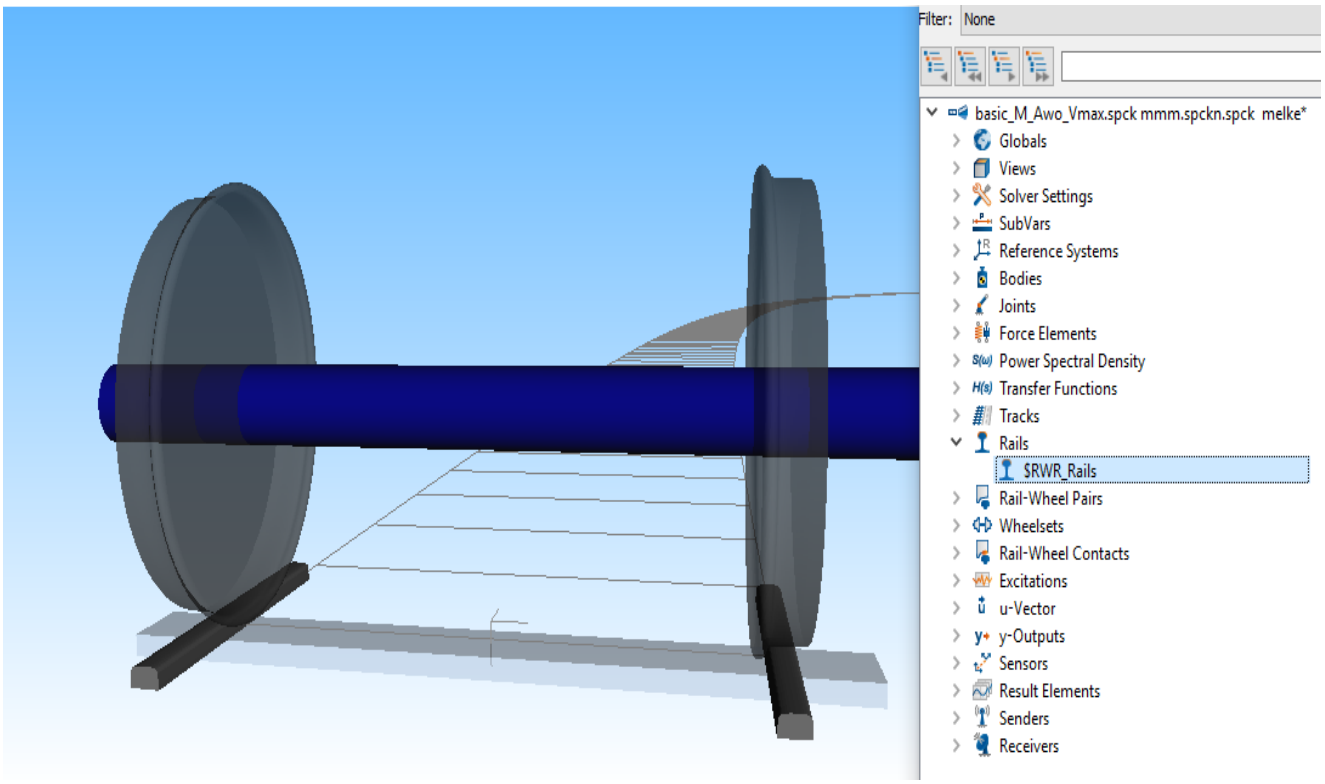

Figure 3.11.1 Standard wheel-rail pair model using SIMPACK 9.8.2

3.12. Track Pair

When each rail–wheel pair is defined, SIMPACK asks to specify the left and right hand contact pairs corresponding to each wheel set. In this way, as can be seen in below, important features as the track gauge and the equivalent conicity are defined. For this project, the value of the equivalent conicity is set to 0.186, being used value in correspondence to the track gauge and type of wheel profile used in this project.

3.13. Rail – Wheel Contacts

The last step concerning the evaluation of the contact problem is the definition of the method to calculate the tangential contact forces and spin contact torque. In SIMPACK library are seven different approaches available and as described earlier the most common rail-wheel contact algorithm in SIMPACK called "FASTSIM" is chosen here.

3.14. Bodies

In order to build up the model, it is necessary to introduce the different geometries that compose the model apart from the wheel sets. This is done with the help of the Body Properties.

By fulfilling the body properties panel (manually of from a specified file) mass, moment of inertia and other properties corresponding to each body of the model are defined. It should be noted that SIMPACK gives the possibility of building a model from multiple sub-models, also called Substructures. In this way, one can create the bogies in a separate SIMPACK file, for example and import the bogies in the main model as substructures to simplify the modeling process.

3.15. Track definition

Once the rail-wheel contact has been totally defined as well as each body composing the model, the next step is the definition of the scenario in which the model will be positioned. In order to do this, a new track has to be created. As can be seen in Figure 3.15.1 Rail track is defined by two tabs

In the first one the user is asked to specify the length and curvature of different sections composing the track in the horizontal plane, as well as the super elevation and the differences in the vertical direction.

The second tab is dedicated to the introduction of the track irregularities, see Figure 3.5. It should be noted that in this work measured track data in lateral, vertical, roll and gauge directions is used as track irregularities in different operational scenarios.

3.16. Static equilibrium and preload calculation

Once the railway model is completely defined along with the scenario, it is time to prepare it for the simulations. With this aim a static initial position must be determined. In such situation, all the derivatives of the state equations (velocities and accelerations) defining the mechanical system are zero. Moreover, special attention must be paid to the elastic force elements present in the model. With the help of the Preload Calculation menu, SIMPACK calculates the value of the preload of every suspension element taking charge of the effect of the gravity on different masses.

In Figure 3.6, the preloads values for each force element can be seen. Moreover, the "Maximum residual acceleration" of the model is also specified in this menu, and of course the corresponding number at the equilibrium position must be equal to zero or very small. For the illustrated case, this value is smaller than 0.012 rad/s2, so can be said that the effect of the gravity is absorbed by the force elements.

Once the force elements are in equilibrium, it is time to determine the equilibrium position of the full model in the three directions. To do so, SIMPACK provides the tool Static Equilibrium which calculates the static position of each body and gives the Maximum force residuum in that position. This value, as in the previous case for the Preload calculation, must be equal to zero or very small. Now, since SIMPACK finds suitable equilibrium positions, the model is ready to be used in the simulations.

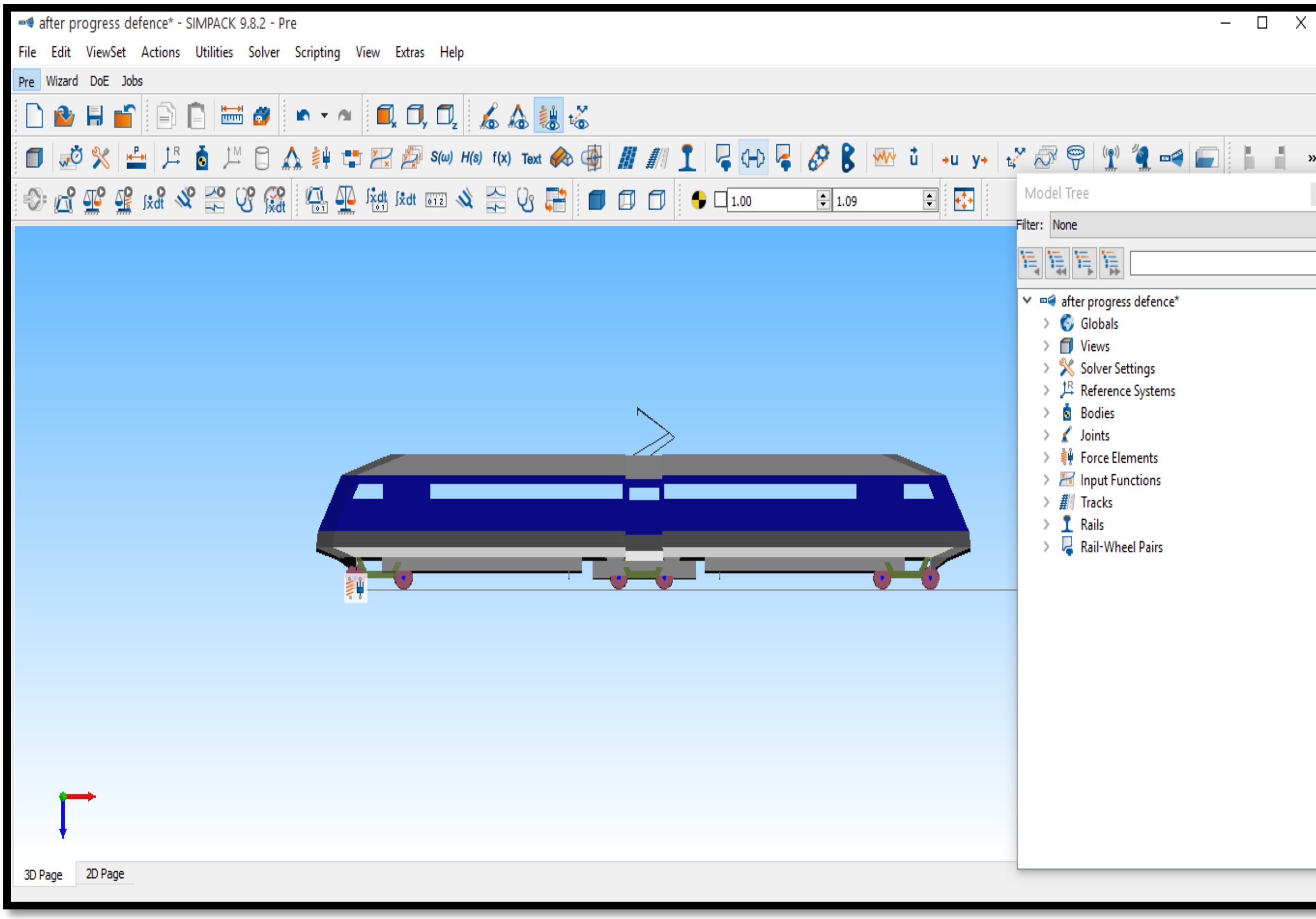

Figure 3.16.1 Rail vehicle and track interaction model by SIMPACK 9.8.2 modeling package

Kalker's Cantact program was applied to the wheel/rail contact, and Fastsim program was utilized to calculate wheel/rail force in model. Meanwhile, elastic track was also considered.

Chapter four

4.1 Simulation Results and discussion

4.1.1. Track parameters

Track parameters describe the characteristics of the track, and track in different conditions and locations may have different representative parameter values. The development of different track parameters is based on many studies which involve complicated measurement. Accurate track parameters give a better understanding of the track system and the selection of track parameters plays an essential role in track model development. In this section, all the important track parameters that are used in the lateral track deterioration model will be presented and described in detail. For validation purpose the track parameters are selected to represent as best as possible.

4.1.2. Track lateral shift model

As described earlier, the algorithm used in the railway model to calculate the tangential forces and the tangential torque is called FASTSIM (A Fast Algorithm for the Simplified Non-Linear Theory of Contact). It is based on the method of Kalker and assumes that the contact patch is elliptical and divided into elements. Thus, calculates the contact forces stresses by a simplified numerical integration. This algorithm has been selected because is well-accepted in vehicle dynamics calculations and more importantly provides fast and reliable results. Note that the spin contact torque is not calculated for the wear analysis. In this section only the track irregularities used during the simulations are explained.

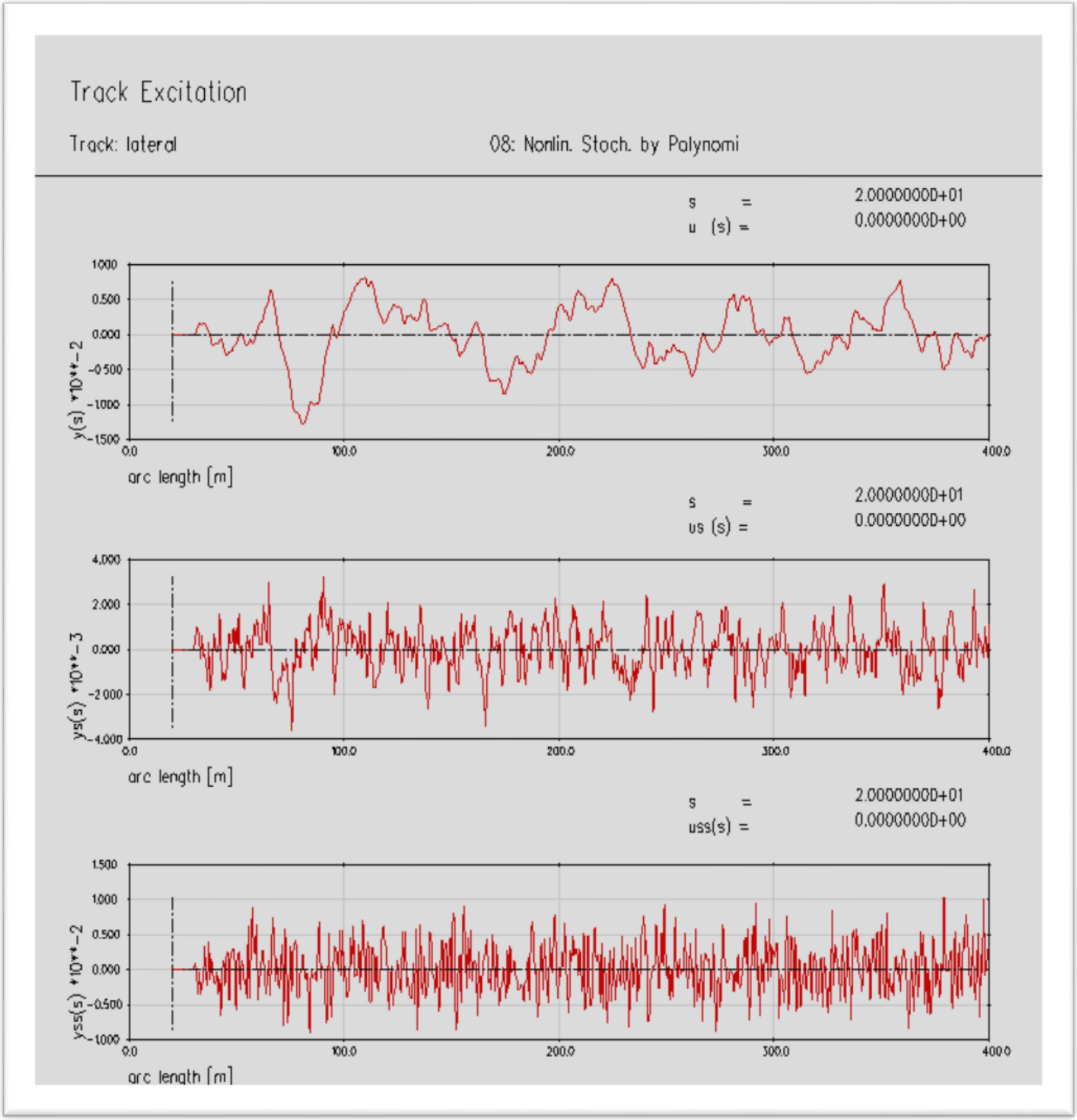

Figure 4.1 Track irregularities in lateral direction and its first and second derivatives

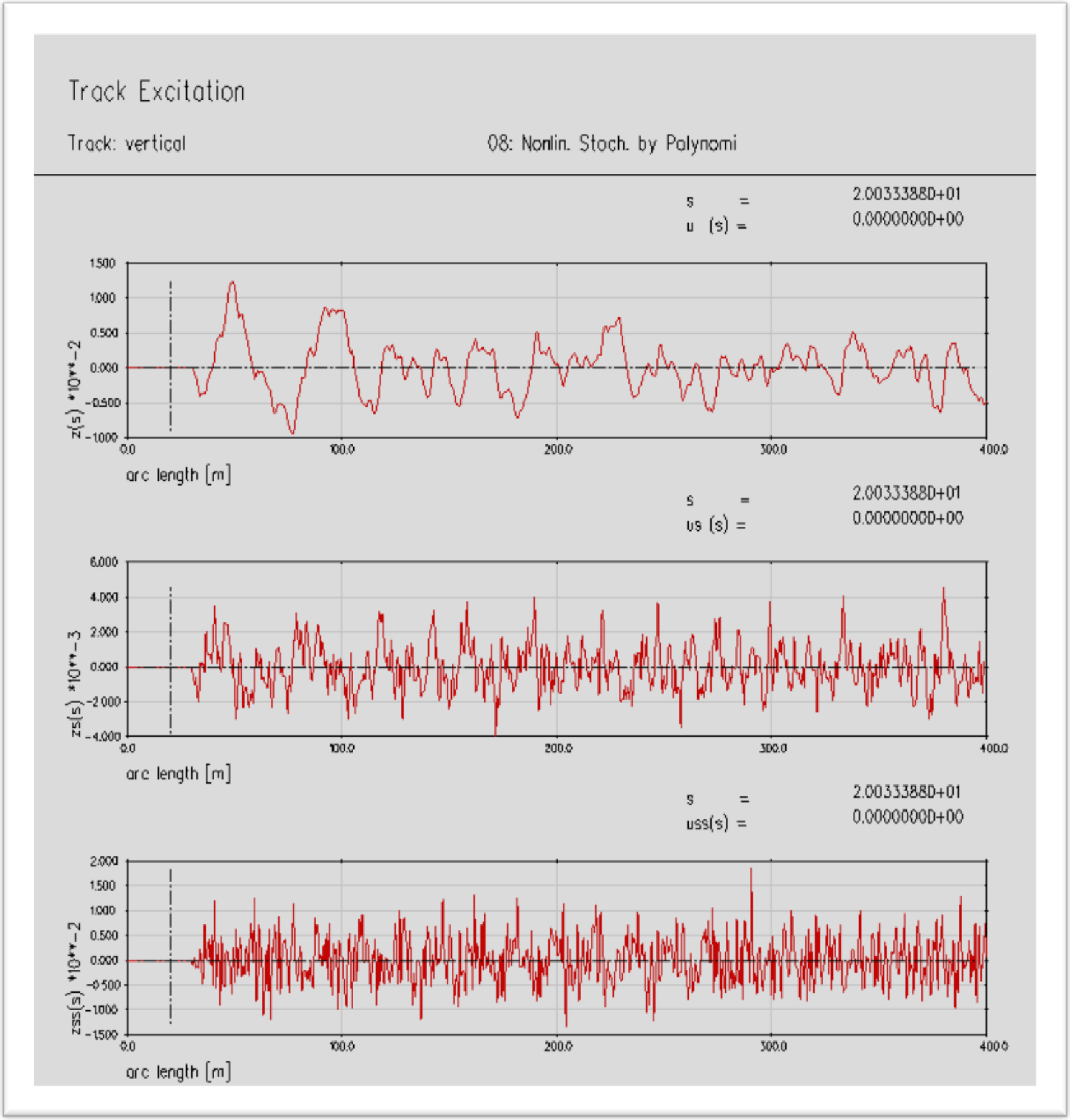

Figure 4.2 Track irregularities in vertical direction and its first and second derivatives

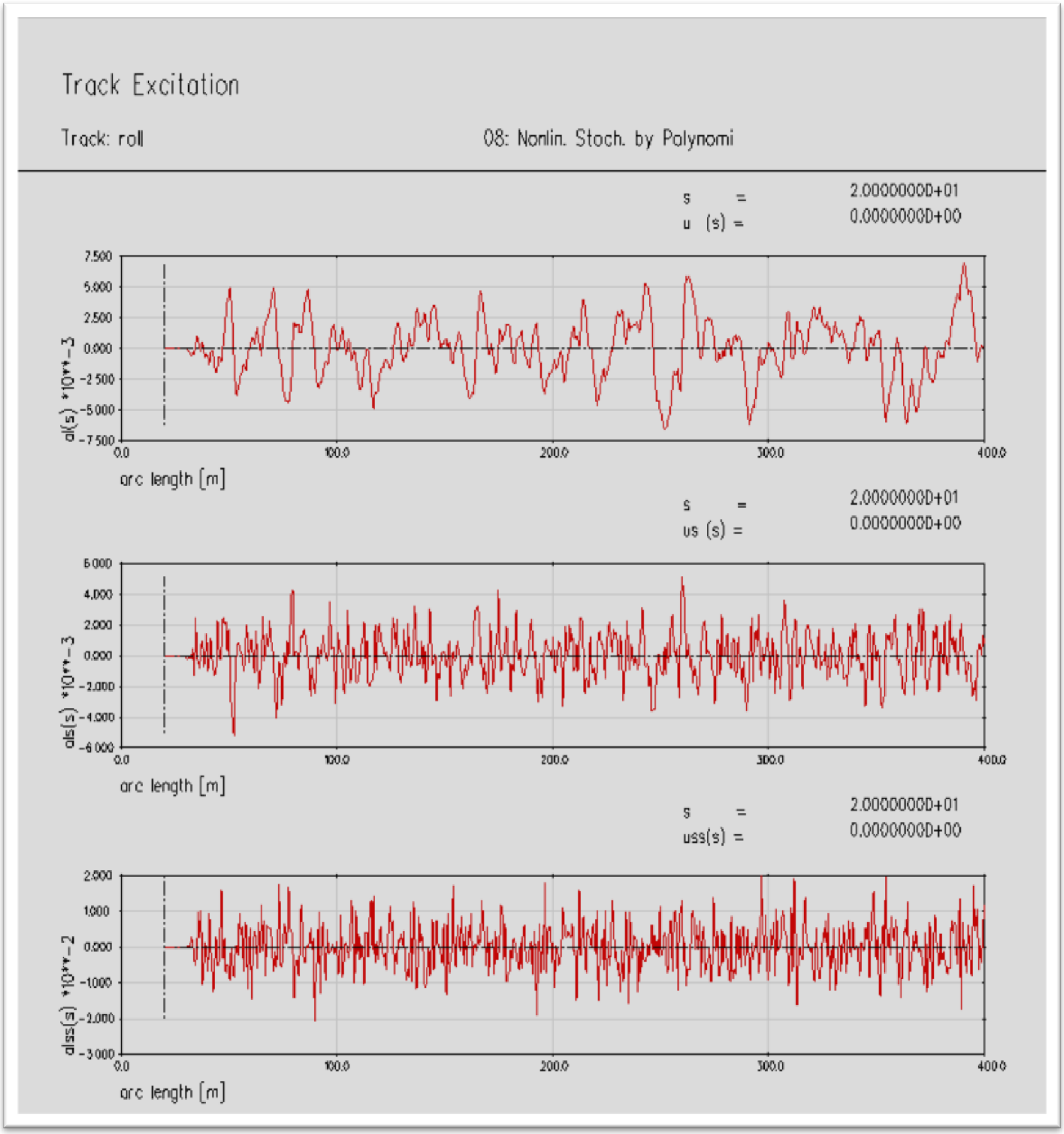

Figure 4.3 Track irregularities in roll direction, its first and second derivatives

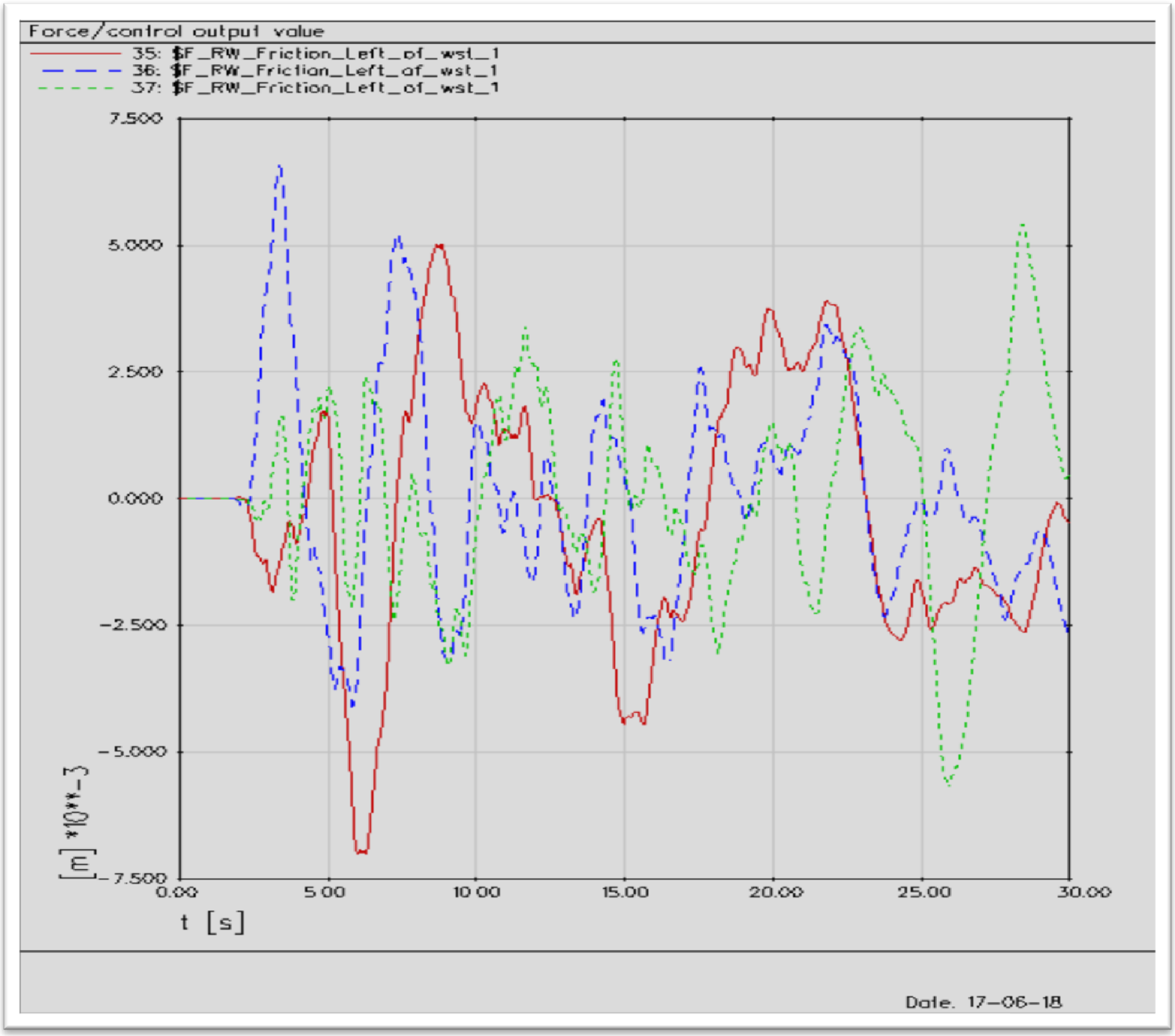

figure 4.4 Track lateral, vertical and roll irregularities a 30 second simulation result

Based on the simulation results all lateral vertical and rolling deviations and their respective derivatives (respective speeds and accelerations of wheel rail contact points) are more sensitive on curved tracks than the straight ones. But the sensitivity of the first two (lateral and vertical) deviations is more responsive to curves than the rolling deviations.

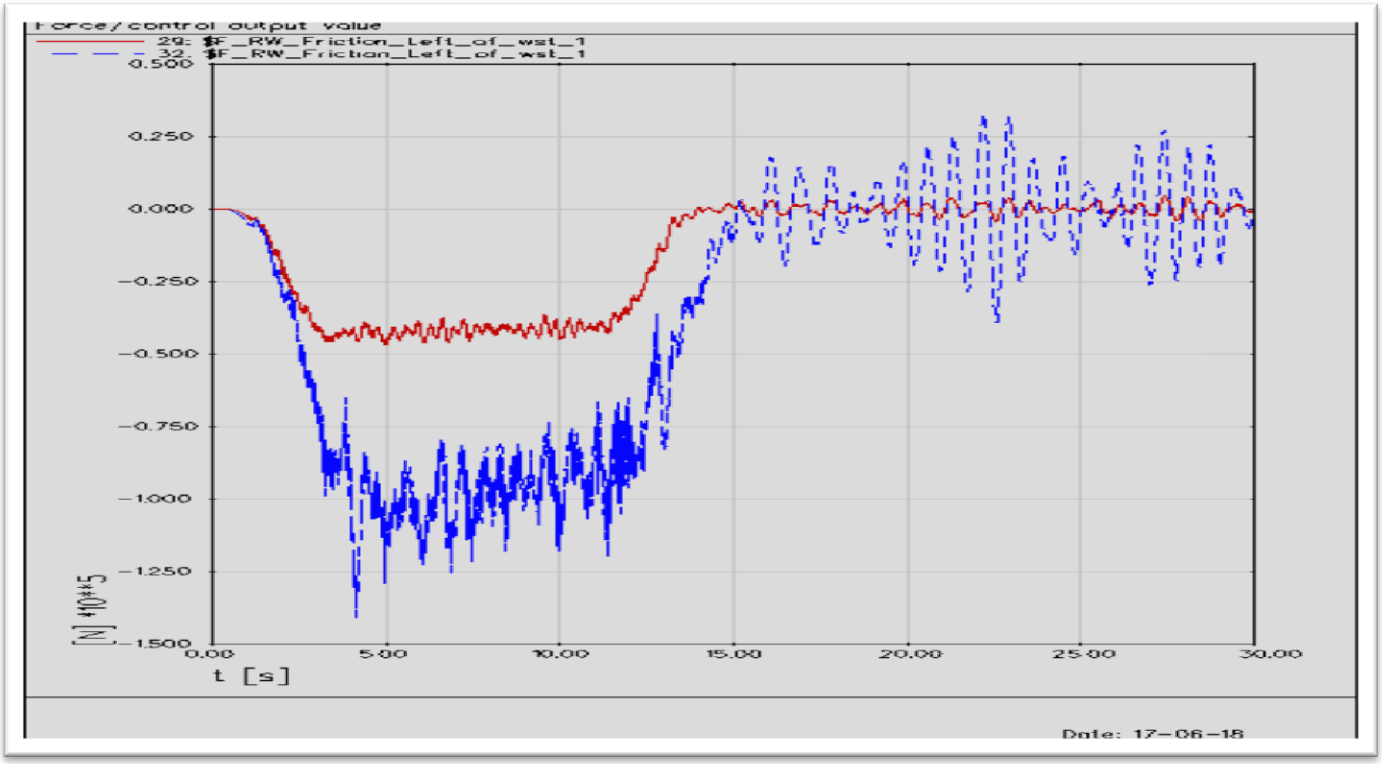

Figure 4.5 lateral forces on track due to wheel loading (red) and vehicle loading (blue) against time

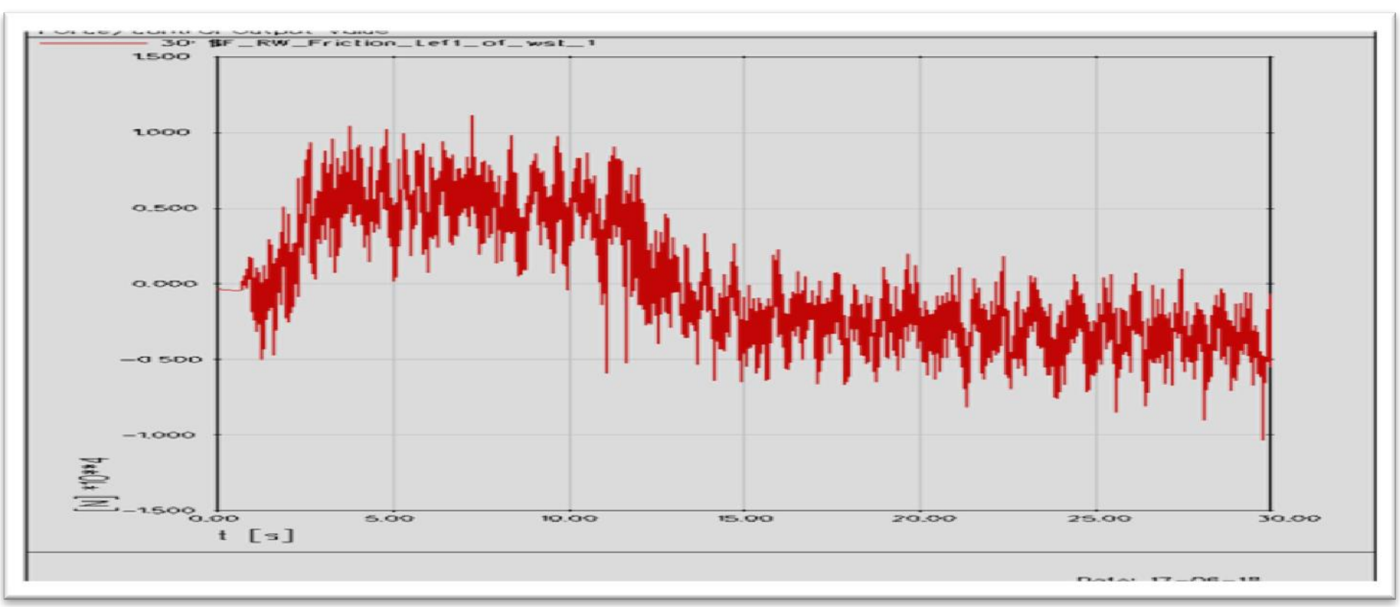

Figure 4.6 wheel vertical loading on track

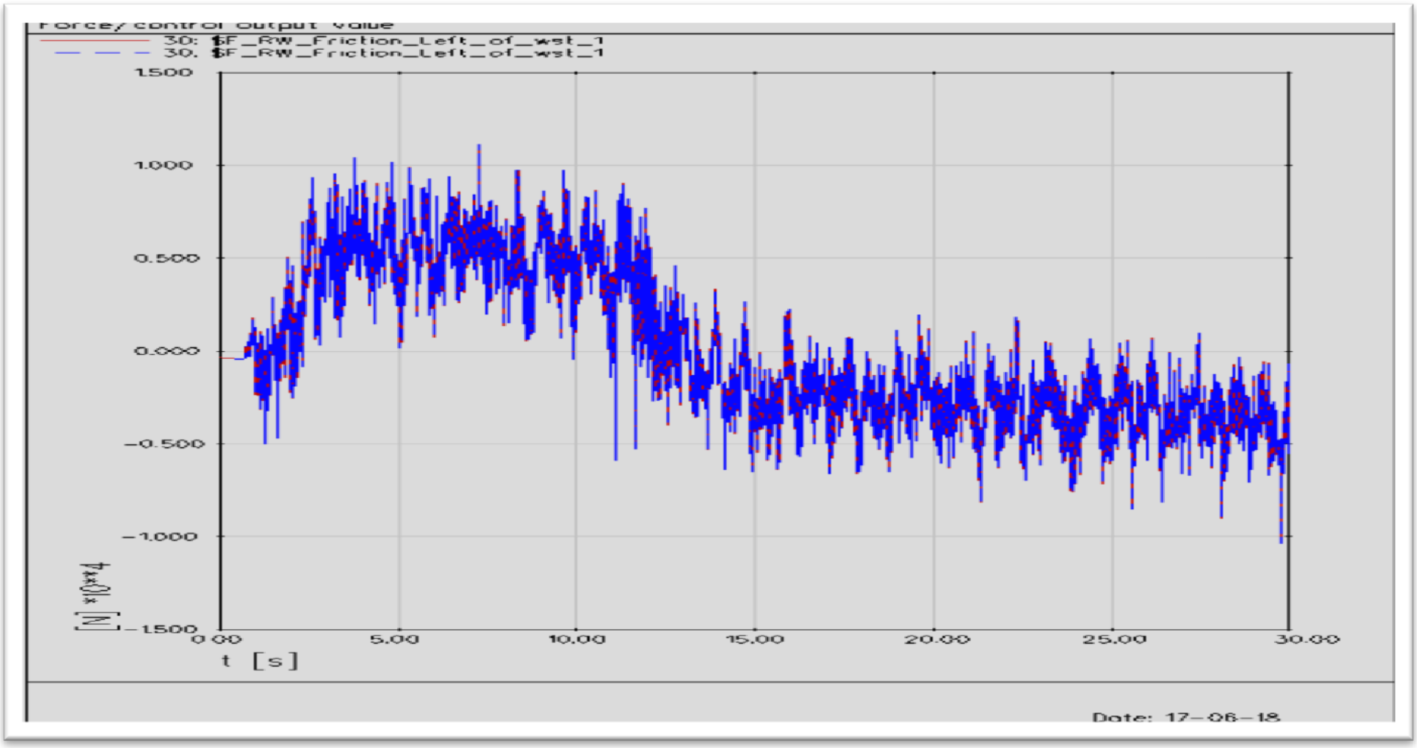

Figure 4.7 vertical forces on track due to wheel loading (red) and vehicle loading (blue)

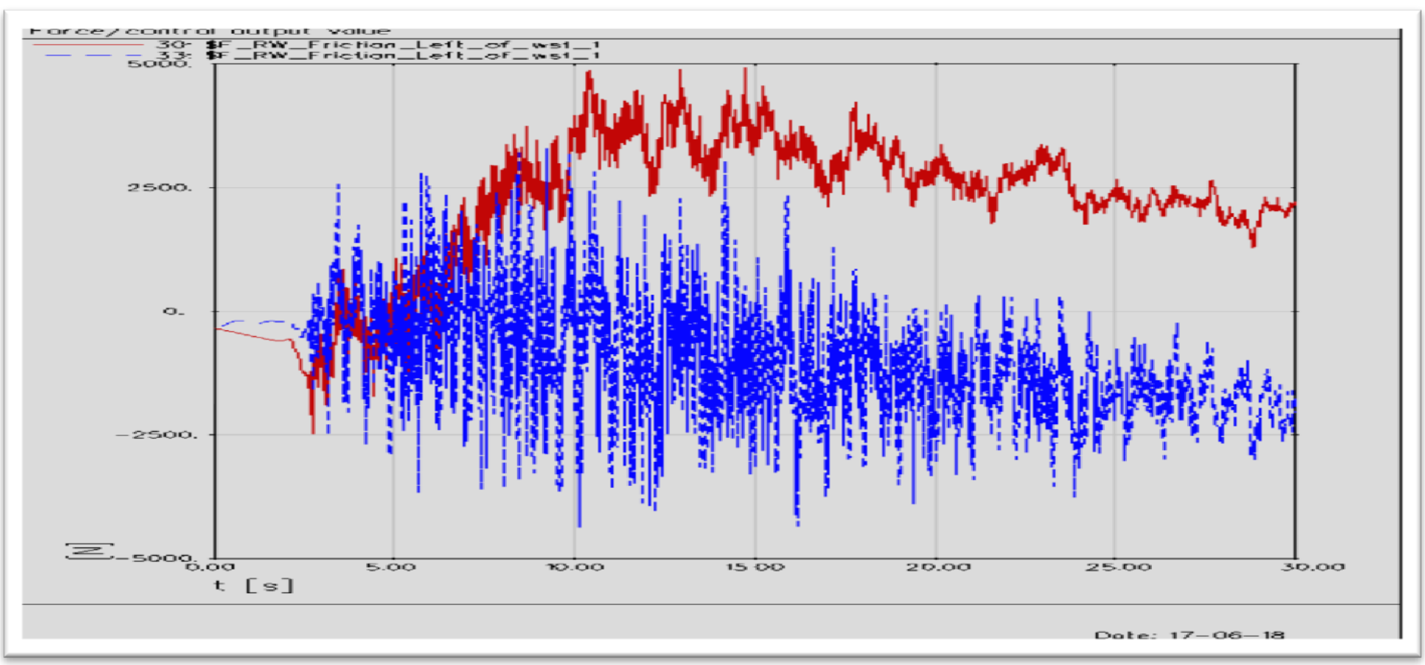

Figure 4.8 Track vertical loading due to wheel forces (red) and vehicle weighting

4.2. Discussion of results

Wear of rail ends are the two major defects in rails. Due to the passage of moving loads and friction between the wheel and the rail, the rail head gets worn-out in the course of service resulting rail surface irregularities. The impact of moving loads, the effect of the forces of acceleration, deceleration, and breaking of wheels, the abrasion due to rail-wheel interaction, the effect of weather conditions such as changes in temperature, snow, and rains, the presence of materials such as sand, the standard of maintenance of the track, and such allied factors causes considerable wear and tear of vertical and lateral planes of the rail head. Lateral wear occurs more on curves because of the lateral thrust exerted on the outer rail by centrifugal force. A lot of the mental of the rail head gets worn out; causing the weight of the rail to decrease .this loss of weight of the rail section should not be such that the stresses exceed their permissible values. When such a stage is reached, rail renewal is called for. In addition, by the limitation of Super elevation there is the possibility of a rail wear. Typical early railway operation resulted in rolling stock being operated at less than equilibrium velocity (all wheels equally sharing the rolling stock weight), or coming to a complete stop on curves. Under such circumstances excess super elevation may lead to a downward force sufficient to damage the inside rail of the curve, or cause derailment of rolling stock toward the center of the curve when draft force is applied to a train. Routine operation of loaded freight trains at low velocity on a curve super elevated to permit operation of higher velocity passenger trains will result in excess wear of the inside rail of the curve by the freight trains.

The AALRT track average irregularity growth rate is calculated and its value is 0.075mm/100days which imply 0.274 mm/year.

The maximum measured lateral and vertical deviation errors are 1.3mm and 1.73mm respectively also the respective minimum values are -0.2mm and -2.5mm and all the maximum values are obtained from the most recent taken data (January 2017).

Since the limited allowable lateral deviation is between -3mm and 5mm, lateral irregularity becomes above the limited value after about 11 years for the lower limit (-3mm) and 14 years of operation for upper limit (5mm). And the maximum track vertical deviation (level difference) is

±6mm implying that the limiting values for both upper and lower limits are met after 16 years of operation.

Therefore the safe operational life of the track dynamic interaction is about 11years and after 11 years the track will be reinstalled on its reverse side to minimize the risk due to irregularities or replaced by new track.

Using SIMPACK MBS package and unworn rail the maximum values of lateral and vertical deviation values are obtained to be about 1.2 mm and 1.4 mm respectively showing that lateral deviation is safer than the vertical ones according to SIMPACK standards. This implies that more attention should be given for vertical alignment especially on straight tracks but on curves the lateral one is too worth nothing.

Both velocity and acceleration parameters of track lateral and vertical components have similar properties with their respective deviations.

Practically the total axel loading capacity value is about 65.9KN which is beyond the maximum design value (63.020KN) has taken during the peak operating hours.

Based on the simulation results all lateral vertical and rolling deviations and their respective derivatives (respective speeds and accelerations of wheel rail contact points) are more sensitive on curved tracks than the straight ones. But the sensitivity of the first two (lateral and vertical) deviations is more responsive to curves than the rolling deviations.

The lateral and vertical forces due to wheel loading and the overall vehicle loading values are curvature dependent and on curves their respective values are much higher than in the non-curved tracks.

Therefore track irregularities are the main concerns of railway projects in curved track sections than the straight track sections and that is why the North-South line of the AALRT is being facing operational problems repeatedly.

Changing the track parameters does not have strong impact on the shape of the track lateral deterioration compared to changes in the vehicle and wheel-rail contact conditions. At a specific location on the track, for example where the peak deflection occurs, the influences of all track parameters are not quite linear due to the resulting dynamic effects. Nonetheless, the RMS of the residual deflection changes appears relatively linear with respect to the track parameter variation. The lateral damage caused by the vehicle depends on both the L/V ratio and the lateral load but it is a complicated dynamic process that cannot easily be expressed through a simple function. It is therefore sensible to establish the damage from different types of vehicle by carrying out vehicle-track dynamic simulations.

It is found that the wheel and rail profiles play a very important role in the development of lateral track deterioration by influencing the lateral dynamics of the vehicle. It is important to choose the correct wheel and rail profiles, and find representative wheel-rail contact conditions for the track section that is being analyzed. A better understanding of rail-wheel wear can lead to a more accurate prediction.

Chapter five

5.1. Conclusions, recommendations and Further Works

The study of vehicle-track lateral dynamic interaction is based on a statistical analysis of track geometry data and vehicle-track dynamic modeling. The work undertaken in this thesis attempts to build a better understanding of track lateral quality characteristics and its deterioration under railway vehicle traffic. This chapter summarizes the achievements made during the research. The track system, the measurements of the track geometry and the definition of the track quality are explained in detail. The background study forms fundamental knowledge for the vehicle-track lateral dynamic interaction study in chapter 1. A review of the current research in the field of vertical and lateral railway track deterioration was presented in Chapter 2 in order to establish a better understanding of track deterioration mechanisms, highlighting the weakness and limitations of these studies.

Based on the background and the reviews done in this field, a statistical analysis and model development are made and simulation analysis are carried out in chapter 3 in order to investigate the relationship between vehicle track lateral and vertical dynamic interactions and track deterioration.

Vehicle dynamics is directly dependent on wheel rail contact and track surface conditions or track irregularities and these parameters are clearly related to time which indicates that after ascertain time value wheel rail contact and track irregularities become worth noting in case of safety, comfort and stability for everything inside the vehicle. Even if there is a schedule for AALRT is being maintained per three months, there are times when continuously maintenance operation is needed even in every month accordingly.

The paper gives a detail information for the characteristics of lateral track irregularities and track deterioration over time. An emphasis is given to the description of lateral and vertical deterioration growth against both curvature and time including lateral and vertical loading behaviors during operation.

5.2. Recommendation

According to the analysis done on the data taken in this paper the minimum time when track irregularity causes problems of transport with AALRT is 11 years. Therefore after 11years the track needs to be either reinstalled on its revers side or be replaced by new tracks to minimize the risks of passengers due to irregularities.

5.3. Further works

It was shown that the track lateral and vertical irregularities are correlated to some extent in both the distance domain and spatial domain. On average the lateral quality is slightly better than the vertical; however there are cases where it can be worse. Due to the limitation of the recorded track data, the lateral track deterioration against the curvature and time are studied separately, so the parameters for these empirical functions are only valid on specific networks. The growth in the standard deviation of the lateral track irregularity against track curvature has only been validated using the AALRT from Stadium to Meshualekia track data, and the growth of the track lateral irregularity SD against time is only validated using a particular section of track data. Further work will be useful to create a more comprehensive equation by combining the curvature and time (or loading cycles) factors, and in addition, the factors that have not been included in this study, such as temperature, ground condition, and traffic etc. To achieve this, additional analysis using measured track data that includes all of the information mentioned above will be required.

Collect track data with comprehensive information, regarding measuring time intervals, curvature ranges, loading tonnage, traffic, temperature, ground condition etc. and establish a more representative empirical equation for lateral and vertical track deterioration.

Conduct an in-depth study into the interface between sleeper and ballast in terms of stiffness and damping values: force-displacement behavior including hysteresis characteristic. Improve and optimize the SIMPACK vehicle models, such improving modeling the tilting mechanism.

Take into account additional factors in the lateral track deterioration model, such as the influence of longitudinal forces from the wheels to the rails, different weather and temperatures, more representative layers of the track bed, uneven stiffness and larger range of wheel-rail contact conditions.

Simplify the lateral track deterioration model by using a distributed vertical load shape function, or by replacing dynamic lateral and vertical forces with representative net vertical and lateral loads.

References

1. Track Technology measurements of track settlment and its prediction with trach dynamic model. **Makoto, I.** 2002, Vol. 16, pp. 15-21.

2. The Effect of Track Geometry on Ride Quality, Industry and General Applications, p. , 1971. **O'Sullivan, K. B. Ullman and W. B.** s.l. : -, 2013, Vol. 11.

3. A short-Range Prediction Model for Track Quality Index,Rail and Rapid Transit. **P. Xu, Q. Sun, R. Liu, and F. Wang.** 2011, Vol. 225.

4. A measurement system for quick rail inspection and effective track maintenance strategy," Mechanical Systems and Signal Processing, . **M. Bocciolone, A. Caprioli, A. Cigada, and A. Collina.** 2007, Vol. 21.

5. **K.Takeshita, E. Yazawa and.** Development of Measurement Device of Track Irregularity using Inertial Mid-chord Offset Method. s.l. : Quarterly report of RTRI, 2012.

6. Track-recording techniques used on British Rail. **Lewis, R. B.** s.l. : IEE Proc, 1984, Vol. 131.

7. Railway Safety and Standards Board. **RSSB, "Railway Group Standard.** 2003, Vols. GC/RT5021,ed.

8. Numerical Simulation Method of Railway Track Irregularity . **Y. H. Liu, F. Li, and Y. H. Huang.** s.l. : Journal of Traffic and Transportation Engineering, 2006, Vol. 6.

9. Power Spectrum Analysis-Modern Tool in The Study of Rail Surface Corrugation . **Massel, A.** s.l. : NDT&E International, 1999., Vol. 32.

10. Dynamics of Railway Vehicle Systems. **Dukkipati, V. K. Garg and R. V.** New York : Academic Press, 1984.

11. Preventing track buckles. **Wolf, G.** s.l. : The Journal of Wheel/Rail Interaction, 2005.

12. **Frederick, C. O.** The Effect of Rail Straightness on Track Maintenance," presented at the Advanced Techniques in Permanent Way Design, Construction and Maintenance. Madrid : s.n., 1981.

13. Ballast Deformation and Track Deterioration, Track Technology of the Next Decade. **Shenton, M. J.** London : Institution of Civil Engineers and held at the University of Nottingham , 1995.

14. The Interaction Between Railway Vehicle Dynamics And Track Lateral Alignment. **Gong, Cencen.** s.l. : University of Huddersfield, 2013.

15. **Kaewunruen, A. M. Remennikov and S.** Investigation of Vibration Characteristics of Prestressed Concrete Sleepers in Free-free and In-situ Conditions. s.l. : Research Online, 2005.

16. Stefens, Identification and development of a model of railway track dynamic behavior . **Dvid, Martyn.** s.l. : Queensland University of Technology, Faculty of Built Environment and Technology , May, 2005.

17. Random Field Modelling of Railway Track Irregularities. **Jaiswal, R. N. Iyengar and O. R.** 1995, Vol. 121.

18. "Numerical Simulation Method of Railway Track Irregularity. **Y. H. Liu, F. Li, and Y. H. Huang.** s.l. : Journal of Traffic and Transportation Engineering, 2006, Vol. 6.

19. Power Spectrum Analysis-Modern Tool in The Study of Rail Surface Corrugation. **Massel, A.** s.l. : NDT&E International, 1999, Vol. 32.

20. Estimation of long wavelength track irregularities from on board measurementS. **Bruni, S. Alfi and S.** s.l. : 2008 4th IET International Conference, 2008.

21. **Werner, K.** Diskrete Riffelabsta und die Suche nach Den Ursachen der Schienenriffeln,. ZEV Classers Annalen 353-359, 1986, Vol. 10.

22. Track Compendium . **Lichtberger, B.** Berlin : Eurail Press, 2005.

23. Rail Corrugation: Characteristics, Gauges and Treatments. **Kalousek, S. L. Grassie and J.** s.l. : Rail and Rapid Transit, pp. 57-58, 1993.

24. Review on rail corrugation studies. **Y. Sato, A. Matsumoto, and K. Knothe,.** s.l. : Wear p. 130, 2002, Vol. 253.

25. Effect of Track Irregularities on Initiation and Evolution of Rail Corrugation. **X. Jin, Z. Wen, and K. Y. Wang.** s.l. : Journal of Sound and Vibration, 2004, Vols. vol. 285, pp. 121148.

26. Short Wavelength Rail Corrugation: Field Trails and Measuring Technology. **Grassie, S. L.** s.l. : Wear, pp. , 1996, Vols. vol. 191, 149-160.

27. DYNAMIC ANALYSIS OF RAILWAY VEHICLE/TRACK INTERACTION FORCES . **HUNT, GEOFFREY A.** s.l. : Doctor of Philosophy of the Loughborough University of Technology , June 1986.

28. Investigationofverticaldynamicbehaviourandmodellingofatypicalindian railroadvehiclethroughbondgraph. **Vivek Kumar, Vikas Rastogi.** Sangrur : Department of Mechanical Engineering, SLIET Longowal, Sangrur, 148106, Punjab, India , April 26 2009.

29. fundamentals of rail vehicle dynamics guidance and stability. **WICKENS, A.H.** loughborough university, UK : SWETS & ZEITLINGER, 2003.

30. **Gillesbie, Thomas D.** Fundamentals of vehicle dynamics. s.l. : Society of Automotive Engineers, Inc. 400 Common welth Drive Wattendale,PA. 15096-0001.

31. A numerical program for railway vehicle-track-structure dynamic interaction using a modal substructuring approach. **Savini, Gabriel.** s.l. : Anno accademico , 2010.

32. TheAnatomyofRailway Vehicle Running Gear. **Boronenko, Anna Orlova and Yuri.** s.l. : Taylor & Francis Group, LLC, 2006.

33. On modelling and dynamical analysis of railway vehicles vibration. **M.Byrtus, V.Zeman, Z.Hlav ac.** s.l. : University of West Bohemia, Department of Mechanics, 2010.

34. SIMULATION DYNAMIC PROCESSES OF RAIL VEHICLE AND RAIL WITH IRREGULARITIES . **Marijonas Bogdevicius, Rasa Zygiene.** Vilniu : KONES Powertrain and Transport, 2014 , Vol. 21.

35. Dynamic studies of railtrack sleepers in a track structure system. **G. Kumaran, Devdas Menon*, K. Krishnan Nair.** Chennai 600 036, India : Journal of Sound and Vibration 268 (2003) 485–501, 2002.

36. Modelling of Railway Vehicle-trackunderground Dynamic Interaction Induced by High-speed Trains. **MARTIN X. D. LI, TORBJÖRN EKEVID, NILS-ERIK WIBERG.** Göteborg, Sweden, : CHALMERS 03:1 , 2003.

37. ReviewofTracksideMonitoringSolutions: FromStrainGages toOpticalFibreSensors. **GeorgesKouroussis, ChristopheCaucheteur, DamienKinet , GeorgiosAlexandrou, OlivierVerlinden, andVéroniqueMoeyaert.** s.l. : sensors ISSN1424-8220 , 2015.

38. **China Railway Group (CRECG) Project manager office for LRT, Ethiopia.** Technical Specifications of Vehicles. July 2013.

39. **Berggren, Eric.** Railway Track Stiffness, Dynamic Measurements and Evaluation for Efficient Maintenance. s.l. : Doctoral Thesis TRITA AVE, 2009.

40. **Chaar, Nizar.** Wheel set Structural Flexibility and Track Flexibility in Vehicle-Track Dynamic Interaction. s.l. : Doctoral Thesis TRITA AVE, 2007.

41. Finite Element Analysis of Slab Track Subjected to Moving Load. **Qingyuan, L. Ping and Z.** s.l. : Journal of Traffic and Transportation Engineering, 2004, Vol. 4.

42. Finite-element Fundamental Theory China Beijing. **Renxian, L.** Guo Fang Gong Ye : s.n., 2009.

43. Fundmentals for Track Lateral Shift for High Speed Rail Applications. **A. Kish, G. Samavedam, and D. Wormely.** - : -, 2004. Vols. -.

44. Modelling the Contact between Wheel and Rail within Multibody System Simulation. **G. SCHUPP, C. WEIDEMANN AND L. MAUER.** Wessling, Germany : INTEC GmbH, 2004.

Appendixes

Appendixes A

ADISS ABABA NS (LINE PHASE 2) LRT PROJECT FROM STUDIUM TO MESUALEKIYA June 2016

ADISS ABABA NS (LINE PHASE 2) LRT PROJECT FROM STUDIUM TO MESUALEKIYA									
NS LINE TRACK CHECKING RECORD JUNE 2016									
NS left	design s.el	site s.el	level	gauge	NS right	design s.el	site s.el	level	gauge
SNZK9+600	1.3	0	0	0	SNYK9+600	9.1	13	3	3
SNZK9+610	21.3	21	22	1	SNYK9+610	29.1	29	0	12
SNZK9+620	40	39	40	11	SNYK9+620	40	40	1	9
SNZK9+630	40	39	39	13	SNYK9+630	40	39	3	11
SNZK9+640	40	39	41	13	SNYK9+640	40	41	2	11
SNZK9+650	40	40	39	12	SNYK9+650	40	41	3	12
SNZK9+660	40	39	40	10	SNYK9+660	40	41	3	15
SNZK9+670	40	33	34	10	SNYK9+670	37.8	38	4	6
SNZK9+680	33.1		8	3	SNYK9+680	17.8	19	4	5
SNZK9+690	13.1	0	-3	3	SNYK9+690	0	2	4	1
SNZK9+700	0	-5	-3	3	SNYK9+700	0	1	4	0
SNZK9+710	0	0	-3	0	SNYK9+710	0	3	4	1
SNZK9+720	0	1	-1	0	SNYK9+720	0	1	2	1
SNZK9+730	0	2	-1	0	SNYK9+730	0	4	3	0
SNZK9+740	0	2	1	1	SNYK9+740	0	2	7	2
SNZK9+750	0	2	-1	2	SNYK9+750	0	3	3	2
SNZK9+760	0	-4	-3	0	SNYK9+760	0	4	3	3
SNZK9+770	0	1	-4	0	SNYK9+770	0	1	5	1
SNZK9+780	0	1	-4	-1	SNYK9+780	0	5	7	-2
SNZK9+790	-12.2	-13	-19	-1	SNYK9+790	-13.1	-7	5	2
SNZK9+800	-32.2	-33	-33	0	SNYK9+800	-33.1	-31	2	0

ADISS ABABA NS (LINE PHASE 2) LRT PROJECT FROM STUDIUM TO MESUALEKIYA									
NS LINE TRACK CHECKING RECORD JUNE 2016									
NS left	design s.el	site s.el	level	gauge	NS right	design s.el	site s.el	level	gauge
SNZK9+810	-50	-53	-54	0	SNYK9+810	-50	-35	14	2
SNZK9+820	-50	-47	-54	0	SNYK9+820	-50	-45	5	1
SNZK9+830	-50	-48	-55	-1	SNYK9+830	-50	-44	9	2
SNZK9+840	-50	-51	-53	0	SNYK9+840	-50	-50	1	0
SNZK9+850	-50	-51	-52	-1	SNYK9+850	-50	-40	11	3
SNZK9+860	-50	-52	-52	0	SNYK9+860	-50	-45	7	2
SNZK9+870	-50	-51	-51	1	SNYK9+870	-50	-45	6	1
SNZK9+880	-50	-49	-53	0	SNYK9+880	-50	-46	7	0
SNZK9+890	-50	-54	-54	-2	SNYK9+890	-50	-44	10	0
SNZK9+900	-50	-52	-52	2	SNYK9+900	-50	-48	5	2
SNZK9+910	-50	-49	-41	2	SNYK9+910	-50	-46	5	0
SNZK9+920	-50	-48	-50	-2	SNYK9+920	-50	-45	7	4
SNZK9+930	-41.1	-44	-64	0	SNYK9+930	-41.2	-47	-3	1
SNZK9+940	-21.2	-21	-4	0	SNYK9+940	-21.2	-18	2	0
SNZK9+950	-1.2	1	0	-1	SNYK9+950	-1.1	1	2	0
SNZK9+960	0	3	-1	0	SNYK9+960	0	3	2	1
SNZK9+970	-6.4	7	-8	-1	SNYK9+970	0	2	2	1
SNZK9+980	-26.3	-25	-27	0	SNYK9+980	16.8	19	2	2
SNZK9+990	-46.3	-46	-48	-2	SNYK9+990	36.8	39	2	1
SNZK10+000	-60	-59	-60	1	SNYK10+000	56.7	57	0	1
SNZK10+010	-60	-60	4E-10	0	SNYK10+010	60	63	3	-1
SNZK10+020	-51.3	-51	0.3	0	SNYK10+020	60	59	-1	0
SNZK10+030	-31.2	-31	0.2	-1	SNYK10+030	44.1	43	-1.1	-1
SNZK10+040	-11.2	-11	0.2	0	SNYK10+040	24.2	25	0.8	-1

ADISS ABABA NS (LINE PHASE 2) LRT PROJECT FROM STUDIUM TO MESUALEKIYA									
NS LINE TRACK CHECKING RECORD JUNE 2016									
NS left	design s.el	site s.el	level	gauge	NS right	design s.el	site s.el	level	gauge
SNZK10+050	0	1	1	-1	SNYK10+050	4.1	6	1.9	-2
SNZK10+060	0	0	0	-1	SNYK10+060	0	2	2	-2
SNZK10+070	0	-1	-1	0	SNYK10+070	0	0	0	-1
SNZK10+080	0	-3	-3	0	SNYK10+080	0	-2	-2	-1
SNZK10+090	0	-3	-3	-1	SNYK10+090	0	0	0	-3
SNZK10+100	0	0	0	0	SNYK10+100	0	1	1	-2
SNZK10+110	0	-2	-2	4	SNYK10+110	0	0	0	-1
SNZK10+120	0	0	0	-1	SNYK10+120	0	0	0	0
SNZK10+130	0	0	0	-1	SNYK10+130	0	0	0	2
SNZK10+140	0	0	0	-2	SNYK10+140	0	-1	-1	-1
SNZK10+150	0	0	0	0	SNYK10+150	0	3	3	1
SNZK10+160	0	0	0	-1	SNYK10+160	0	2	2	0
SNZK10+170	0	0	0	0	SNYK10+170	0	-1	-1	0
SNZK10+180	0	2	2	0	SNYK10+180	0	0	0	0
SNZK10+190	-8.5	-13	-4.5	-1	SNYK10+190	0	1	1	-3
SNZK10+200	-28.5	-33	-4.5	0	SNYK10+200	11	12	1	0
SNZK10+210	-48.5	-50	-1.5	-1	SNYK10+210	31	31	5E-11	-1
SNZK10+220	-50	-60	-10	-1	SNYK10+220	51	49	-2	-1
SNZK10+230	-50	-60	-10	-2	SNYK10+230	60	58	-2	0
SNZK10+240	-40.9	-43	-2.1	0	SNYK10+240	60	57	-3	0
SNZK10+250	-20.9	-21	-0.1	-1	SNYK10+250	50.4	49	-1.4	0
SNZK10+260	-0.9	3	3.9	-1	SNYK10+260	30.4	35	4.6	0
SNZK10+270	0	3	3	-1	SNYK10+270	10.4	14	3.6	-1
SNZK10+280	0	2	2	0	SNYK10+280	0	2	2	1

ADISS ABABA NS (LINE PHASE 2) LRT PROJECT FROM STUDIUM TO MESUALEKIYA									
NS LINE TRACK CHECKING RECORD JUNE 2016									
NS left	design s.el	site s.el	level	gauge	NS right	design s.el	site s.el	level	gauge
SNZK10+290	0	1	1	0	SNYK10+290	0		0	
SNZK10+300	0	0	0	1	SNYK10+300	0		0	
SNZK10+310	0	0	0	0	SNYK10+310	0	-2	-2	2
SNZK10+320	0	0	0	0	SNYK10+320	0	1	1	0
SNZK10+330	0	1	1	0	SNYK10+330	0	2	2	0
SNZK10+340	0	1	1	1	SNYK10+340	0	4	4	-1
SNZK10+350	0	1	1	1	SNYK10+350	0	3	3	-3
SNZK10+360	0	0	0	2	SNYK10+360	0	0	0	-1
SNZK10+370	0	0	0	-1	SNYK10+370	0	1	1	2
SNZK10+380	0	0	0	0	SNYK10+380	0	-2	-2	-3
SNZK10+390	0	3	3	0	SNYK10+390	0	0	0	-2
SNZK10+400	0	1	1	1	SNYK10+400	0	3	3	-1

ADISS ABABA NS (LINE PHASE 2) LRT PROJECT FROM STUDIUM TO MESUALEKIYA October 2016

ADISS ABABA NS (LINE PHASE 2) LRT PROJECT FROM STUDIUM TO MESUALEKIYA									
NS LINE TRACK CHECKING RECORD OCTOBER 2016									
NS left	design s.el	site s.el	level	gauge	NS right	design s.el	site s.el	level	gauge
SNZK9+600	1.3	0	0	0	SNYK9+600	10	13	3	3
SNZK9+610	21.3	21	22	1	SNYK9+610	29	29	0	12
SNZK9+620	40	39	40	11	SNYK9+620	39	40	1	9
SNZK9+630	40	39	39	13	SNYK9+630	36	39	3	11
SNZK9+640	40	39	41	13	SNYK9+640	39	41	2	11
SNZK9+650	40	40	39	12	SNYK9+650	38	41	3	12
SNZK9+660	40	39	40	10	SNYK9+660	38	41	3	15

ADISS ABABA NS (LINE PHASE 2) LRT PROJECT FROM STUDIUM TO MESUALEKIYA									
NS LINE TRACK CHECKING RECORD OCTOBER 2016									
NS left	design s.el	site s.el	level	gauge	NS right	design s.el	site s.el	level	gauge
SNZK9+670	40	33	34	10	SNYK9+670	34	38	4	6
SNZK9+680	33.1		8	3	SNYK9+680	15	19	4	5
SNZK9+690	13.1	0	-3	3	SNYK9+690	-2	2	4	1
SNZK9+700	0	-5	-3	3	SNYK9+700	-3	1	4	0
SNZK9+710	0	0	-3	0	SNYK9+710	-1	3	4	1
SNZK9+720	0	1	-1	0	SNYK9+720	-1	1	2	1
SNZK9+730	0	2	-1	0	SNYK9+730	1	4	3	0
SNZK9+740	0	2	1	1	SNYK9+740	-5	2	7	2
SNZK9+750	0	2	-1	2	SNYK9+750	0	3	3	2
SNZK9+760	0	-4	-3	0	SNYK9+760	1	4	3	3
SNZK9+770	0	1	-4	0	SNYK9+770	-4	1	5	1
SNZK9+780	0	1	-4	-1	SNYK9+780	-2	5	7	-2
SNZK9+790	-12.2	-13	-19	-1	SNYK9+790	-12	-7	5	2
SNZK9+800	-32.2	-33	-33	0	SNYK9+800	-33	-31	2	0
SNZK9+810	-50	-53	-54	0	SNYK9+810	-49	-35	14	2
SNZK9+820	-50	-47	-54	0	SNYK9+820	-50	-45	5	1
SNZK9+830	-50	-48	-55	-1	SNYK9+830	-53	-44	9	2
SNZK9+840	-50	-51	-53	0	SNYK9+840	-51	-50	1	0
SNZK9+850	-50	-51	-52	-1	SNYK9+850	-51	-40	11	3
SNZK9+860	-50	-52	-52	0	SNYK9+860	-52	-45	7	2
SNZK9+870	-50	-51	-51	1	SNYK9+870	-51	-45	6	1
SNZK9+880	-50	-49	-53	0	SNYK9+880	-53	-46	7	0
SNZK9+890	-50	-54	-54	-2	SNYK9+890	-54	-44	10	0
SNZK9+900	-50	-52	-52	2	SNYK9+900	-53	-48	5	2
SNZK9+910	-50	-49	-41	2	SNYK9+910	-51	-46	5	0

ADISS ABABA NS (LINE PHASE 2) LRT PROJECT FROM STUDIUM TO MESUALEKIYA									
NS LINE TRACK CHECKING RECORD OCTOBER 2016									
NS left	design s.el	site s.el	level	gauge	NS right	design s.el	site s.el	level	gauge
SNZK9+920	-50	-48	-50	-2	SNYK9+920	-52	-45	7	4
SNZK9+930	-41.1	-44	-64	0	SNYK9+930	-44	-47	-3	1
SNZK9+940	-21.2	-21	-4	0	SNYK9+940	-20	-18	2	0
SNZK9+950	-1.2	1	0	-1	SNYK9+950	-1	1	2	0
SNZK9+960	0	3	-1	0	SNYK9+960	1	3	2	1
SNZK9+970	-6.4	7	-8	-1	SNYK9+970	0	2	2	1
SNZK9+980	-26.3	-25	-27	0	SNYK9+980	17	19	2	2
SNZK9+990	-46.3	-46	-48	-2	SNYK9+990	37	39	2	1
SNZK10+000	-60	-59	-60	1	SNYK10+000	57	57	0	1
SNZK10+010	-60	-60	4E-10	0	SNYK10+010	60	63	3	-1
SNZK10+020	-51.3	-51	0.3	0	SNYK10+020	60	59	-1	0
SNZK10+030	-31.2	-31	0.2	-1	SNYK10+030	44.1	43	-1.1	-1
SNZK10+040	-11.2	-11	0.2	0	SNYK10+040	24.2	25	0.8	-1
SNZK10+050	0	1	1	-1	SNYK10+050	4.1	6	1.9	-2
SNZK10+060	0	0	0	-1	SNYK10+060	0	2	2	-2
SNZK10+070	0	-1	-1	0	SNYK10+070	0	0	0	-1
SNZK10+080	0	-3	-3	0	SNYK10+080	0	-2	-2	-1
SNZK10+090	0	-3	-3	-1	SNYK10+090	0	0	0	-3
SNZK10+100	0	0	0	0	SNYK10+100	0	1	1	-2
SNZK10+110	0	-2	-2	4	SNYK10+110	0	0	0	-1
SNZK10+120	0	0	0	-1	SNYK10+120	0	0	0	0
SNZK10+130	0	0	0	-1	SNYK10+130	0	0	0	2
SNZK10+140	0	0	0	-2	SNYK10+140	0	-1	-1	-1
SNZK10+150	0	0	0	0	SNYK10+150	0	3	3	1

ADISS ABABA NS (LINE PHASE 2) LRT PROJECT FROM STUDIUM TO MESUALEKIYA									
NS LINE TRACK CHECKING RECORD OCTOBER 2016									
NS left	design s.el	site s.el	level	gauge	NS right	design s.el	site s.el	level	gauge
SNZK10+160	0	0	0	-1	SNYK10+160	0	2	2	0
SNZK10+170	0	0	0	0	SNYK10+170	0	-1	-1	0
SNZK10+180	0	2	2	0	SNYK10+180	0	0	0	0
SNZK10+190	-8.5	-13	-4.5	-1	SNYK10+190	0	1	1	-3
SNZK10+200	-28.5	-33	-4.5	0	SNYK10+200	11	12	1	0
SNZK10+210	-48.5	-50	-1.5	-1	SNYK10+210	31	31	5.1E-11	-1
SNZK10+220	-50	-60	-10	-1	SNYK10+220	51	49	-2	-1
SNZK10+230	-50	-60	-10	-2	SNYK10+230	60	58	-2	0
SNZK10+240	-40.9	-43	-2.1	0	SNYK10+240	60	57	-3	0
SNZK10+250	-20.9	-21	-0.1	-1	SNYK10+250	50.4	49	-1.4	0
SNZK10+260	-0.9	3	3.9	-1	SNYK10+260	30.4	35	4.6	0
SNZK10+270	0	3	3	-1	SNYK10+270	10.4	14	3.6	-1
SNZK10+280	0	2	2	0	SNYK10+280	0	2	2	1
SNZK10+290	0	1	1	0	SNYK10+290	0		0	
SNZK10+300	0	0	0	1	SNYK10+300	0		0	
SNZK10+310	0		0		SNYK10+310	0	-2	-2	2
SNZK10+320	0		0		SNYK10+320	0	1	1	0
SNZK10+330	0	1	1	0	SNYK10+330	0	2	2	0
SNZK10+340	0	1	1	1	SNYK10+340	0	4	4	-1
SNZK10+350	0	1	1	1	SNYK10+350	0	3	3	-3
SNZK10+360	0	0	0	2	SNYK10+360	0	0	0	-1
SNZK10+370	0	0	0	-1	SNYK10+370	0	1	1	2
SNZK10+380	0	0	0	0	SNYK10+380	0	-2	-2	-3
SNZK10+390	0	3	3	0	SNYK10+390	0	0	0	-2

ADISS ABABA NS (LINE PHASE 2) LRT PROJECT FROM STUDIUM TO MESUALEKIYA									
NS LINE TRACK CHECKING RECORD OCTOBER 2016									
NS left	design s.el	site s.el	level	gauge	NS right	design s.el	site s.el	level	gauge
SNZK10+400	0	1	1	1	SNYK10+400	0	3	3	-1

ADISS ABABA NS (LINE PHASE 2) LRT PROJECT FROM STUDIUM TO MESUALEKIYA January 2017

ADISS ABABA NS (LINE PHASE 2) LRT PROJECT FROM STUDIUM TO MESUALEKIYA									
NS LINE TRACK CHECKING RECORD									
NS left	design s.el	site s.el	level	gauge	NS right	design s.el	site s.el	level	gauge
SNZK9+600	1.3	0	-1.3	0	SNYK9+600	10	13	3	3
SNZK9+610	21.3	22	0.7	1	SNYK9+610	29	29	0	12
SNZK9+620	40	40	3.6E-11	11	SNYK9+620	39	40	1	9
SNZK9+630	40	39	-1	13	SNYK9+630	36	39	3	11
SNZK9+640	40	41	1	13	SNYK9+640	39	41	2	11
SNZK9+650	40	39	-1	12	SNYK9+650	38	41	3	12
SNZK9+660	40	40	3.6E-11	10	SNYK9+660	38	41	3	15
SNZK9+670	40	34	-6	10	SNYK9+670	34	38	4	6
SNZK9+68	33.1	8	-25.1	3	SNYK9+68	15	19	4	5

ADISS ABABA NS (LINE PHASE 2) LRT PROJECT FROM STUDIUM TO MESUALEKIYA									
NS LINE TRACK CHECKING RECORD									
NS left	design s.el	site s.el	level	gauge	NS right	design s.el	site s.el	level	gauge
0					0				
SNZK9+690	13.1	-3	-16.1	3	SNYK9+690	-2	2	4	1
SNZK9+700	0	-3	-3	3	SNYK9+700	-3	1	4	0
SNZK9+710	0	-3	-3	0	SNYK9+710	-1	3	4	1
SNZK9+720	0	-1	-1	0	SNYK9+720	-1	1	2	1
SNZK9+730	0	-1	-1	0	SNYK9+730	1	4	3	0
SNZK9+740	0	1	1	1	SNYK9+740	-5	2	7	2
SNZK9+750	0	-1	-1	2	SNYK9+750	0	3	3	2
SNZK9+760	0	-3	-3	0	SNYK9+760	1	4	3	3
SNZK9+770	0	-4	-4	0	SNYK9+770	-4	1	5	1
SNZK9+780	0	-4	-4	-1	SNYK9+780	-2	5	7	-2
SNZK9+790	-12.2	-19	-6.8	-1	SNYK9+790	-12	-7	5	2
SNZK9+80	-32.2	-33	-0.8	0	SNYK9+80	-33	-31	2	0

ADISS ABABA NS (LINE PHASE 2) LRT PROJECT FROM STUDIUM TO MESUALEKIYA									
NS LINE TRACK CHECKING RECORD									
NS left	design s.el	site s.el	level	gauge	NS right	design s.el	site s.el	level	gauge
0					0				
SNZK9+810	-50	-54	-4	0	SNYK9+810	-49	-35	14	2
SNZK9+820	-50	-54	-4	0	SNYK9+820	-50	-45	5	1
SNZK9+830	-50	-55	-5	-1	SNYK9+830	-53	-44	9	2
SNZK9+840	-50	-53	-3	0	SNYK9+840	-51	-50	1	0
SNZK9+850	-50	-52	-2	-1	SNYK9+850	-51	-40	11	3
SNZK9+860	-50	-52	-2	0	SNYK9+860	-52	-45	7	2
SNZK9+870	-50	-51	-1	1	SNYK9+870	-51	-45	6	1
SNZK9+880	-50	-53	-3	0	SNYK9+880	-53	-46	7	0
SNZK9+890	-50	-54	-4	-2	SNYK9+890	-54	-44	10	0
SNZK9+900	-50	-52	-2	2	SNYK9+900	-53	-48	5	2
SNZK9+910	-50	-41	9	2	SNYK9+910	-51	-46	5	0
SNZK9+92	-50	-50	1.8E-	-2	SNYK9+92	-52	-45	7	4

ADISS ABABA NS (LINE PHASE 2) LRT PROJECT FROM STUDIUM TO MESUALEKIYA									
NS LINE TRACK CHECKING RECORD									
NS left	design s.el	site s.el	level	gauge	NS right	design s.el	site s.el	level	gauge
0			10		0				
SNZK9+930	-41.1	-64	-22.9	0	SNYK9+930	-44	-47	-3	1
SNZK9+940	-21.2	-4	17.2	0	SNYK9+940	-20	-18	2	0
SNZK9+950	-1.2	0	1.2	-1	SNYK9+950	-1	1	2	0
SNZK9+960	0	-1	-1	0	SNYK9+960	1	3	2	1
SNZK9+970	-6.4	-8	-1.6	-1	SNYK9+970	0	2	2	1
SNZK9+980	-26.3	-27	-0.7	0	SNYK9+980	17	19	2	2
SNZK9+990	-46.3	-48	-1.7	-2	SNYK9+990	37	39	2	1
SNZK10+000	-60	-60	-5E-11	1	SNYK10+000	57	57	0	1
SNZK10+010	-60	-60	0	0	SNYK10+010	60	59	-1	1
SNZK10+020	-51	-51	0	-1	SNYK10+020	60	56	-4	2
SNZK10+030	-31	-32	-1	-2	SNYK10+030	44	41	-3	1
SNZK10+0	-11	-10	1	-1	SNYK10+0	24	23	-1	1

ADISS ABABA NS (LINE PHASE 2) LRT PROJECT FROM STUDIUM TO MESUALEKIYA									
NS LINE TRACK CHECKING RECORD									
NS left	design s.el	site s.el	level	gauge	NS right	design s.el	site s.el	level	gauge
40					40				
SNZK10+050	0	0	0	1	SNYK10+050	4	3	-1	2
SNZK10+060	0	-1	-1	0	SNYK10+060	0	-1	-1	0
SNZK10+070	0	-2	-2	0	SNYK10+070	0	-1	-1	1
SNZK10+080	0	-3	-3	-1	SNYK10+080	0	-3	-3	0
SNZK10+090	0	-2	-2	0	SNYK10+090	0	-4	-4	0
SNZK10+100	0	0	0	0	SNYK10+100	0	-3	-3	0
SNZK10+110	0	-2	-2	0	SNYK10+110	0	-4	-4	1
SNZK10+120	0	1	1	-1	SNYK10+120	0	-4	-4	2
SNZK10+130	0	0	0	-1	SNYK10+130	0	-3	-3	1
SNZK10+140	0	1	1	0	SNYK10+140	0	-4	-4	0
SNZK10+150	0	0	0	-2	SNYK10+150	0	-4	-4	0
SNZK10+1	0	0	0	-1	SNYK10+1	0	-1	-1	3

ADISS ABABA NS (LINE PHASE 2) LRT PROJECT FROM STUDIUM TO MESUALEKIYA									
NS LINE TRACK CHECKING RECORD									
NS left	design s.el	site s.el	level	gauge	NS right	design s.el	site s.el	level	gauge
60					60				
SNZK10+170	0	0	0	-1	SNYK10+170	0	-6	-6	0
SNZK10+180	0	0	0	0	SNYK10+180	0	1	1	3
SNZK10+190	-8	-10	-2	0	SNYK10+190	0	-1	-1	1
SNZK10+200	-28	-22	6	-1	SNYK10+200	11	11	0	1
SNZK10+210	-48	-48	0	-1	SNYK10+210	31	29	-2	0
SNZK10+220	-50	-50	0	-2	SNYK10+220	51	47	-4	0
SNZK10+230	-50	-52	-2	-2	SNYK10+230	60	58	-2	1
SNZK10+240	-41	-42	-1	0	SNYK10+240	60	57	-3	2
SNZK10+250	-21	-21	0	-2	SNYK10+250	50	48	-2	2
SNZK10+260	-1	-1	0	-2	SNYK10+260	30	29	-1	1
SNZK10+270	0	-1	-1	-2	SNYK10+270	10	10	0	0
SNZK10+2	0	-1	-1	-2	SNYK10+2	0	0	0	2

ADISS ABABA NS (LINE PHASE 2) LRT PROJECT FROM STUDIUM TO MESUALEKIYA									
NS LINE TRACK CHECKING RECORD									
NS left	design s.el	site s.el	level	gauge	NS right	design s.el	site s.el	level	gauge
80					80				
SNZK10+290	0	0	0	0	SNYK10+290	0	0	0	0
SNZK10+300	0	0	0	-1	SNYK10+300	0	0	0	0
SNZK10+310	0	0	0	0	SNYK10+310	0	-7	-7	3
SNZK10+320	0	0	0	0	SNYK10+320	0	3	3	1
SNZK10+330	0	3	3	0	SNYK10+330	0	0	0	1
SNZK10+340	0	3	3	2	SNYK10+340	0	1	1	0
SNZK10+350	0	-2	-2	-1	SNYK10+350	0	1	1	-1
SNZK10+360	0	-1	-1	0	SNYK10+360	0	-3	-3	4
SNZK10+370	0	-5	-5	-2	SNYK10+370	0	-1	-1	0
SNZK10+380	0	1	1	-1	SNYK10+380	0	-2	-2	1
SNZK10+390	0	-1	-1	0	SNYK10+390	0	-2	-2	2
SNZK10+4	0	1	1	0	SNYK10+4	0	1	1	2

ADISS ABABA NS (LINE PHASE 2) LRT PROJECT FROM STUDIUM TO MESUALEKIYA									
NS LINE TRACK CHECKING RECORD									
NS left	design s.el	site s.el	level	gauge	NS right	design s.el	site s.el	level	gauge
00					00				

APPENDIXES B

Wheel lateral loading on track

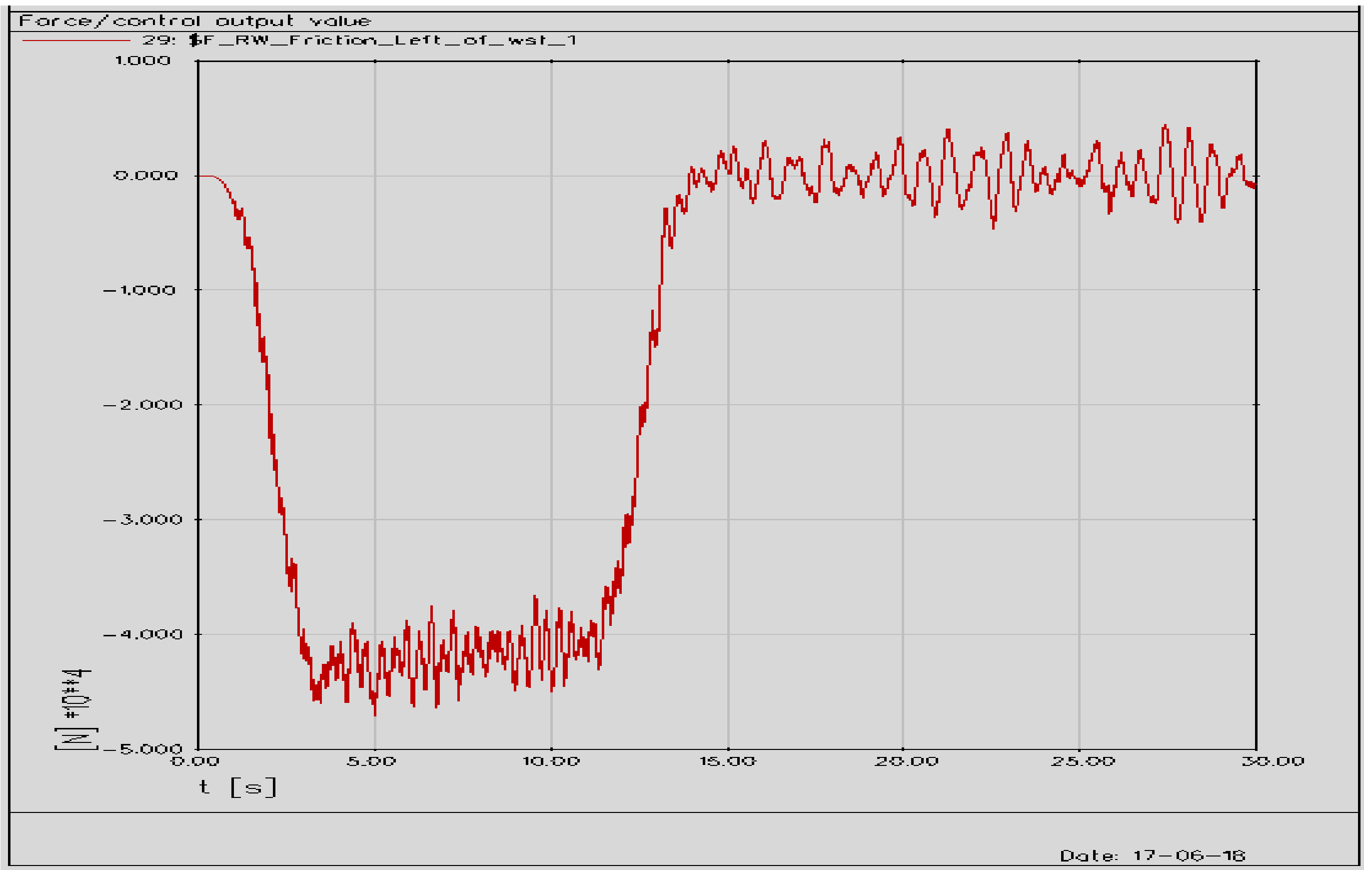

Lateral to vertical wheel loading ratio on track

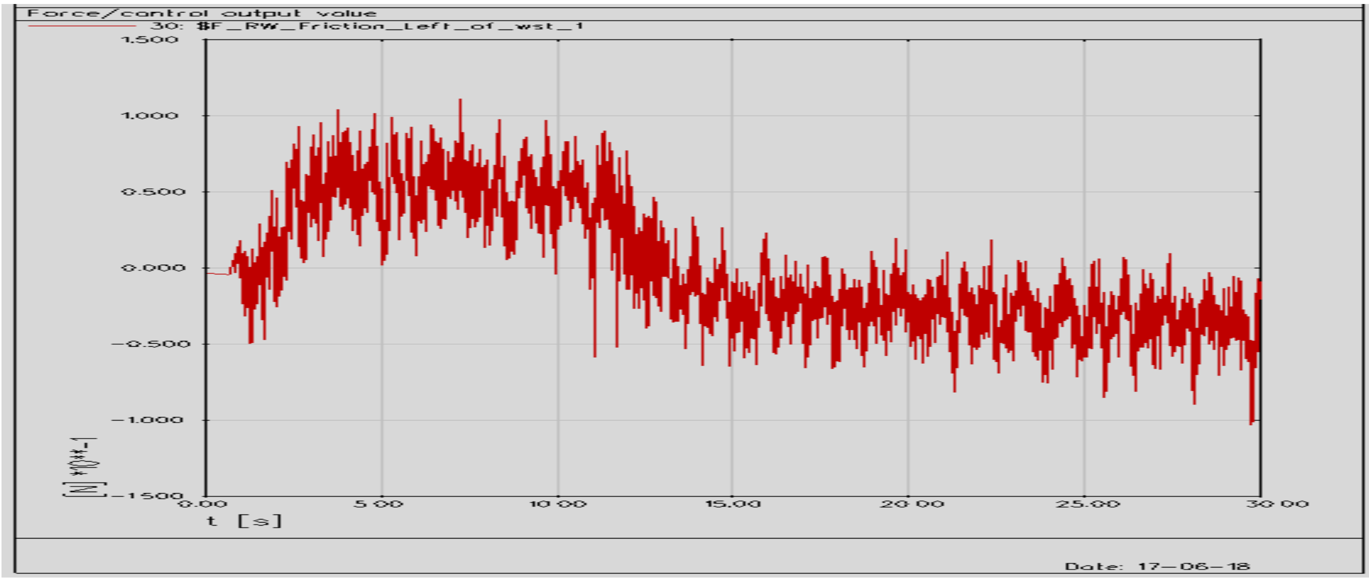

Lateral loading on track due to wheel force (red graph) and vehicle weighting (blue graph) a 30 second simulation